Title
Genomic study of Plasmodium falciparum gene regulation and mechanisms of drug action and resistance

Author
Shock, Jennifer Leigh

Publication Date
2008-07-28

Peer reviewed|Thesis/dissertation

Genomic study of *Plasmodium falciparum* gene regulation and mechanisms of drug action and resistance

by

Jennifer Leigh Shock

DISSERTATION

Submitted in partial satisfaction of the requirements for the degree of

DOCTOR OF PHILOSOPHY

in

BIOCHEMISTRY

in the

GRADUATE DIVISION

of the

UNIVERSITY OF CALIFORNIA, SAN FRANCISCO

[redacted]

Acknowledgements

I would like to acknowledge my advisor, Dr. Joseph DeRisi for his guidance, encouragement and enthusiasm during my graduate work. His support and interest in my future plans is also greatly appreciated.

I would also like to acknowledge the people who participated in the work done throughout this dissertation. Kael Fischer is not only extremely knowledgeable, but also a patient teacher, and helped me through all of the data analysis in Chapter 2. Erica Dahl did many of the preliminary and follow up experiments for Chapter 3, and stayed positive even when our paper had been rejected.

I would definitely like to thank the DeRisi lab for their support through all of the good and bad times of graduate school. I would especially like to thank Manuel Llinás, Z.B. Bozdech and Edith Wong for all their friendship and guidance when I first joined the lab. I would also like to thank Charlie Kim, Polly Fordyce and Matt Miller for their friendship and guidance as I'm leaving.

Lastly, I would like to thank my friends and family for helping me through six years of grad school. My parents have been supportive through the whole process and have never pestered me about when I will be done. My sister Terry has been there every step of the way, and knows exactly what it is like to be a grad student at UCSF. And of course Hetty Fan, Billy Rowell, Brad Zuchero, Megan Bergkessel and Oliver Liu whose friendships have meant the world to me.

Genomic study of *Plasmodium falciparum* gene regulation and mechanisms of drug action and resistance

Jennifer Leigh Shock

Abstract

Plasmodium falciparum, the causative agent of the deadliest type of human malaria continues to be a major cause of morbidity and mortality in many parts of the world. Because of the difficult nature of genetic and biochemical manipulations in *P. falciparum* genomic approaches are an increasingly important tool for studying this organism. We applied genomic approaches to learn about three distinct aspects of *P. falciparum* biology: mRNA decay during the intraerythrocytic developmental cycle (IDC), the antimalarial mechanism of tetracycline antibiotics, and the relationship between chloroquine resistance and mutations in the *P. falciparum* chloroquine resistance transporter (PfCRT).

To study mRNA decay in *P. falciparum*, we used a genome-wide approach to characterize the decay profile of every gene in the genome during the IDC. We found that half-lives for all genes increased during the IDC, indicating that life-cycle is a major determinant of decay rate in *P. falciparum*. We also found that specific variations in decay patterns were superimposed upon the dominant trend of progressive half-life lengthening. These variations in decay pattern were frequently enriched for genes with specific cellular functions or processes, making gene function a secondary determinant of decay rate.

Next, we used genomic techniques to study the antimalarial mechanism of action of tetracycline antibiotics. Using DNA microarrays to characterize the transcriptome over two generations after treatment with doxycycline, we found that expression of apicoplast genes is specifically inhibited, even if the drug was removed after the first generation. This inhibition is likely caused by a disruption of apicoplast function as evidenced by a block in apicoplast genome replication, a lack of processing of an apicoplast-targeted protein, and failure to elongate and segregate during schizogony.

Lastly, to study chloroquine resistance mediated by mutations in PfCRT we used *Saccharomyces cerevisiae* as a heterologous system to begin characterizing the structure-function relationship of PfCRT. We used DNA microarrays to find yeast genes which respond in a dose-dependent manner to chloroquine. These genes will be a starting point towards building a platform for characterizing resistance profiles of new 4-amino-quinoline drugs.

Table of Contents

List of Tables

List of Figures

Chapter 2

Chapter 3

Chapter 4

Appendix

Introduction

Plasmodium falciparum, one of the four species of *Plasmodium* that cause malaria in humans, kills over one million people each year [1]. Despite efforts by a number of global health organizations, deaths due to malaria have actually increased over the last decade [2]. Widespread drug resistance to the most commonly used drugs is partially responsible for this ongoing burden, which highlights the importance of seeking out new targets and new classes of antimalarials.

P. falciparum has an interesting and complex life-cycle. Infection in the human host begins with the bite of an infected mosquito where sporozoites are injected into the host from the mosquito salivary gland. These sporozoites then use a type of gliding motility to make their way into the blood stream, and then into the liver. Once in the liver, sporozoites invade and traverse through Kupffer cells and several hepatocytes before settling on a hepatocyte to grow in. The parasite makes a parasitophorous vacuole and begins to de-differentiate from the motile sporozoite into a trophozoite like stage. The parasite then rapidly divides to produce a large number of merozoites which are released into the blood stream and go on to invade red blood cells.

Once in red blood cells, parasites proceed through a 48 hour life cycle with several distinct morphological stages. Parasites begin in the ring stage, progress to the metabolically active trophozoite stage and then undergo schizogony to produce more merozoites which can then invade more red blood cells. This stage is responsible for all of the clinical symptoms associated with malaria infection. The synchronous release of parasites causes recurring fevers and eventually anemia. In severe malaria, sequestration

of the parasites in blood vessels or in specific organs can cause splenomegaly, kidney and liver failure, seizures, coma and even death.

During this intraerythrocytic developmental cycle (IDC), some parasites branch off this pathway to produce male and female gametocytes. When a mosquito bites an infected human, the male and female gametocytes differentiate into microgametes and macrogametes respectively. In the mosquito midgut, the flagellated microgametes fertilize the macrogamete to produce an ookinete. This ookinete then traverses the midgut wall and forms an oocyst which grows and divides to produce thousands of sporozoites. These sporozoites then make their way to the mosquito's salivary glands where the whole cycle repeats itself.

It is expected that the parasite uses gene regulation to help facilitate the changes from one host to another, and one morphological stage to another. However, many aspects of gene regulation that are well understood in model organisms are not understood in *Plasmodium* and may be quite different. The completion of the *Plasmodium falciparum* genome in 2002 and the subsequent sequencing of several other important *Plasmodium* species including *P. vivax*, *P. yoelii*, *P. berghei*, *P. chabaudi*, and *P. knowlesi* has offered many insights into parasite biology and pathogenesis. However, there is currently a limited understanding of basic biology in *Plasmodium*, making it difficult to capitalize on this wealth of information. The time consuming and laborious nature of biochemical and genetic manipulation in *P. falciparum* also adds to the difficulty in doing research in this organism. Consequently, a different approach is needed.

In the past five years, several labs have used microarrays to measure steady-state levels of RNA throughout the IDC, as well as the sexual stages, some mosquito stages and the liver stages of parasite growth [3-6]. Microarrays can also be used to measure response to drug pressure and to measure other aspects of gene regulation such as splicing and mRNA decay [7-9]. Using microarrays can give a wealth of information without requiring massive amounts of parasite culture.

This thesis describes three applications using microarrays to study *P. falciparum* biology: one in which microarrays are used to measure mRNA decay rates through the IDC, one in which microarrays are used to determine the effects of antibiotic pressure, and one in which yeast microarrays are used as a preliminary step to study the structure-function relationship of the *P. falciparum* chloroquine resistance transporter (PfCRT).

mRNA decay in *Plasmodium falciparum*

Previously, several labs have used microarrays to measure steady-state RNA levels in various *P. falciparum* life stages [3-6]. In these studies, it was found that most genes encoded in the *P. falciparum* genome appear to be highly regulated. During the intraerythrocytic life cycle (IDC), genes appear to be regulated by the cell cycle, being turned on once when needed, and then turned off [3, 4]. Specific genes also appear to be upregulated during the gametocyte, sporozoite, oocyst and liver stages [5, 6, 10].

The genome has revealed that the basic machinery required for basal transcription, splicing, transport, translation and mRNA decay are present in the genome. However, it appears that many specific transcription factors are either absent or highly diverged [11, 12]. It has also been difficult to identify specific sequence motifs important

for controlling transcription due to the low complexity of the extremely A/T rich genome, although recently more progress has been made in this area [13-15]. Regardless, this seeming lack of similarity to well studied systems makes it difficult to use our understanding of gene regulation from organisms such as *Saccharomyces cerevisiae* as a framework for understanding transcription in this highly diverged parasite.

The apparent absence of much of the basic machinery required for transcriptional regulation has led many researchers to hypothesize that post-transcriptional regulation plays an important role in *P. falciparum*. Post-transcriptional regulation encompasses many different processes including mRNA splicing, transport, localization, decay and translational repression. Although over 50% of *P. falciparum* genes contain one or more introns, very little is known about the role of splicing and alternative splicing on gene regulation and, virtually nothing is known about the role of mRNA transport or localization.

Some work has been done on translational repression, which indicates that it is important in the transition from the human host to the mosquito vector [16]. Transcripts of several genes in the female gametocyte are held in a complex with a Dhh1p homolog DOZI, and are translationally repressed until the gametocytes were ingested by mosquitoes. Translational repression is then lifted as the parasites develop into female gametes. However, it is not known if translational repression plays a major role in gene regulation during the IDC.

I chose to focus my graduate work on the role of mRNA decay in *P. falciparum*, an important although often underappreciated aspect of gene regulation. The amount of steady-state RNA available for translation is the result of the rate of transcription offset

by the rate of decay. In fact several microarray studies in other organisms found that in response to cellular signals 40-50% of changes in RNA level were due to mRNA decay [17, 18]. Currently, there is very little known about the components of mRNA decay in *P. falciparum*, and few of the proteins involved in mRNA decay were correctly annotated by the original sequencing effort.

Two major pathways for the degradation of mRNA, both of which are deadenylation dependent have been identified from work in mammals and *S. cerevisiae* [19]. The first step of each mRNA decay pathway is deadenylation. In one pathway, deadenylation is followed by decapping and then 5' to 3' decay, and in the other it is followed by 3' to 5' decay. Although these pathways are clearly distinct, they exhibit functional redundancy: knocking out non-essential components of either pathway has only a minimal affect on the transcriptome in yeast [20, 21]. *P. falciaparum* has orthologs to most of the components identified from other organisms, with a few exceptions noted below.

The initial deadenylation step is carried out by 3' exonucleases specific for the poly(A) tail, and is thought to be the rate-limiting step of mRNA decay [22]. This step is also the only reversible step in that substrates can be readenylated and removed from the decay pathway [23]. The major deadenylase in mammalian cells is PARN, an RNase D homolog that is conserved in many eukaryotes. In *S. cerevisiae*, deadenylation is carried out by two complexes: Pan2p/Pan3p and Ccr4p/Pop2p. The Ccr4p/Pop2p complex is the dominant deadenylase in yeast, and is part of a much larger complex called the Ccr4/Not complex, which also has roles in transcription initiation and elongation and protein modification, suggesting the possibility that these processes are coregulated [19, 24]. *P.*

falciparum has orthologs to both the Ccr4p/Pop2p complex and PARN, but not Pan2p/Pan3p.

Following deadenylation, transcripts can be degraded via one of two distinct pathways. In 5' to 3' decay, Dcp1p and Dcp2p decap the transcript leaving the 5' end available for exonucleolytic decay. There are also a number of enhancers and regulators of decapping including Edc1p-3p, the Lsm complex and the DEAD box helicase Dhh1p. After decapping, subsequent degradation of the transcript proceeds through Xrn1p, the major 5' to 3' exonuclease. Eukaryotes also possess a related exonuclease called Rat1p, which is thought to function mainly in the nucleus.

In 3' to 5' decay, transcripts are degraded by the exosome, a large complex comprised of 9 or 10 essential proteins depending on the organism. Many of these proteins have a 3' to 5' exonuclease domain, but it has recently become clear that in yeast, Rrp44p is the only catalytic subunit [25, 26]. In humans, Rrp41p also has weak activity on its own [26]. An eleventh component, Rrp6p, is associated with the exosome only in the nucleus and is not essential but has shown exonuclease activity [26]. Orthologs for Rrp43p, Rrp46p and Mtr3p have not yet been identified in *P. falciparum*. Interestingly, these same proteins were difficult to identify in *Trypanosoma brucei* as well, but homologs were eventually identified through association with the other exosome components [27, 28]. Because these proteins are expected to play mainly a structural role, it is possible they are highly diverged and have only weak homology in their respective nuclease domains.

Also associated with the exosome are two helicases thought to be involved in regulation and substrate specificity: Ski2p and Mtr4p. Lastly, the free 5' methyl cap

generated by 3' to 5' decay is hydrolyzed by a cap scavenger, Dcs1p. This protein has also been difficult to identify in *P. falciparum.*

The numerous factors that make up the finely tuned decay machinery regulate the decay rates of every transcript made in the cell. The complexity of the system allows for many possible avenues of regulation, including interactions between specific RNA binding proteins and motifs in the 3' UTRs of transcripts, developmental regulation of decay components, and localization of factors or RNAs to specific compartments in the cell such as P bodies [29]. Any of these methods of regulation are possible in *P. falciparum*. In particular, developmental regulation of decay components is an attractive model considering that many of the putative decay components in *P. falciparum* are transcriptionally regulated during the IDC, with peak expression during the ring to early trophozoite stages.

In the eukaryotic organisms studied so far, the specific half-life of each mRNA is precisely related to its physiological role and in many cases can be altered in response to different stimuli or developmental conditions [29-32]. For example, it was found in yeast that core metabolic genes such as those encoding glycolytic enzymes produce mRNAs with very long half-lives, yet genes encoding components of the mating type signaling pathway produce mRNAs with very short half-lives. However, it is still largely not understood how this regulation is achieved.

Previously, decay rates had not been determined for any *P. falciparum* transcripts, nor had any of the mRNA decay components been genetically or biochemically characterized. Given the importance of mRNA decay in overall gene regulation, we conducted a genome-wide study of mRNA decay in *P. falciparum* using a microarray-

based approach to measure mRNA half-life as a function of the IDC which is described in Chapter 2.

We found that the overall rates of mRNA decay change during the IDC. The developmental cycle begins with very short half-lives in the ring stage and progresses through the cycle with longer and longer half-lives until in the late schizont stage, the half-lives are very long and very broadly distributed. We also found that like other organisms studied so far the functional category of the mRNAs themselves are also a factor in the rate of decay, although to a lesser extent. A genome-wide change in mRNA decay rate during a development cycle has not been observed in any other organism to date.

Antibiotics which target the apicoplast cause a delayed death phenotype in *Plasmodium falciparum*

A range of antibiotics have been used successfully for both prophylaxis and treatment of malaria. Many antibiotics already have established safety and toxicity profiles and are relatively inexpensive, making them attractive candidates for antimalarial use.

One drawback to many of these antibiotics is that they exhibit what has been termed delayed death in their action against *Plasmodium.* In patients, these drugs show a long lag before clearance of parasites, and *in vitro* it has been shown that these drugs have a dramatic increase in potency when treatment of parasites is extended from one to two generations. Although this phenomenon was first reported more than 20 years ago,

there is still disagreement about which drugs cause delayed death and why this phenomenon occurs [33].

It is generally agreed that tetracycline, doxycycline, clindamycin and chloramphenicol, which are all inhibitors of prokaryotic translation cause delayed death (table 1). It is generally but not universally thought that thiostrepton which also inhibits translation does not cause delayed death. There is no agreement about whether ciprofloxacin, a DNA replication inhibitor, and rifampin, a transcription inhibitor, cause delayed or immediate death.

Many of the differences in these studies can be explained by differences in the strains used to assess drug efficacy. Several studies which tested multiple strains find a high degree of strain to strain variability, including one study which found IC_{50}s for doxycycline ranging from 0.7 to 108μM among 71 strains after 48 hours of treatment [34-36]. Treatment after 96 hours gave IC_{50}s which were 4-5 times lower but with a similarly broad range [35].

Another possible reason for the differences seen from study to study could be the different assays used to determine IC_{50}s. Although most of the assays used test for inhibition of growth, the timing and assays used vary widely. Some studies determined the number of parasites after treatment by looking at DNA content at a single endpoint using sybr green or YOYO1 [34, 37]. Other studies used hypoxanthine uptake for anywhere from 18 to 48 hours to determine growth inhibition [33, 36, 38, 39]. One study, which used both hypoxanthine uptake and staining with YOYO1 to determine IC_{50}s, reported up to four fold differences depending on the method used [40].

A better understanding of the mechanism behind the delayed death phenomenon would help clear up many of these inconsistencies. All the drugs known to cause delayed death inhibit housekeeping functions in prokaryotes such as DNA replication, transcription and translation [41]. Because *Plasmodium* is a eukaryotic parasite, it was not known how these drugs worked, but it was speculated that they might inhibit the parasite mitochondria. However, in the last 10-15 years it has become clear that like plants, *Plasmodium* and other apicomplexans have both a mitochondria and a plastid like organelle called an apicoplast [42]. Although still controversial, there is mounting evidence that the target of most antibiotics in *Plasmodium* is the apicoplast.

The apicoplast was most likely acquired by secondary endosymbiosis of a red or green algae [43]. It has a 35 kb circular genome with a minimal but complete set of tRNAs, rRNAs and ribosomal proteins which can translate the genes on the circle [44]. It also encodes some subunits of a bacterial RNA polymerase and has been shown to be both transcriptionally and translationally active [44, 45]. Aside from the genes involved in transcription and translation, there are only two genes on the plastid. One is a *clpC* homolog believed to be involved in transporting and or folding proteins in the plastid. The other is a homolog of *sufB* in prokaryotes and its function remains largely unknown but may be involved in iron-sulfur cluster biogenesis [42, 46].

Antibiotics effective against *Plasmodium* are now thought to primarily target the apicoplast, and possibly to some extent the mitochondria [41, 47]. The mechanism of action of these antibiotics are well characterized in bacteria and can be grouped into inhibitors of DNA replication, transcription or translation.

Inhibitors of DNA replication

Circular genomes like that of the *Plasmodium* plastid require a type II topoisomerase to untangle supercoiled DNA during replication [48, 49]. Type II topoisomerases work by passing the tangled pieces of DNA through a double stranded cut and then resealing the cut. Ciprofloxacin inhibits topoisomerases by stabilizing the transient topoisomerase-DNA intermediate, preventing resealing which results in linearization.

Both subunits of a bacterial type II topoisomerase are found in the nucleus of *Plasmodium* and the *gyrA* subunit is sensitive to ciprofloxacin [50]. Treatment with ciprofloxacin causes cleavage of the plastid genome, but not of the nuclear genome [48]. Treatment with ciprofloxacin has also been shown to cause a 10 fold reduction of plastid genome copy number after 48 hours of drug treatment in *Toxoplasma gondii*, indicating inhibition of DNA replication [51].

Inhibitors of Transcription

Transcription in the plastid is accomplished using the typical $\alpha_2\beta\beta'\sigma$ RNA polymerase subunits, and the plastid has been shown to be transcriptionally active [41]. The *Plasmodium* plastid encodes *rpoB* and *rpoC,* while the *rpoA* and *rpoD* genes are in the nucleus. Rifampin is a specific inhibitor of the β subunit of bacterial RNA polymerase and is active against *Plasmodium in vitro* and *in vivo* [52].

Despite the efficacy of rifampin, it is still unclear whether plastid transcription is the target of this drug. Two reports that treatment with rifampin specifically inhibit *rpoBC* transcription within 6 hours indicate that rifampin acts on plastid transcription [53,

54]. However, reports that treatment with rifampin rapidly inhibits total protein and nucleic acid synthesis would suggest that the target is not the plastid [52]. Perhaps the most telling data are that strains selected for rifampin resistance do not carry mutations in the *rpoB* gene, which would be expected if it were the target and is a common mechanism of resistance in bacteria [52]. Further work is needed to identify the mechanism of action for rifampin and to determine if it truly targets the plastid.

Inhibitors of Translation

Many antibiotics that inhibit 70S ribosomes, including clindamycin, erythromycin, azithromycin, thiostrepton, tetracycline, doxycycline and minocycline, show antimalarial activity. All but thiostrepton are universally agreed to exhibit delayed death when used to treat *Plasmodium* parasites.

Thiostrepton is a thiopeptide antibiotic that inhibits translation by binding to the GTPase pocket on the large subunit rRNA and inhibiting GTPase activity. The sequence requirements for thiostrepton binding are well characterized and while the plastid rRNA is predicted to be sensitive, the nuclear and mitochondrial rRNAs should be resistant [54, 55]. Thiostrepton has been shown to bind *Plasmodium* ribosomal plastid RNA with ten times greater affinity than nuclear rRNA [55]. In addition to evidence of direct binding, treatment with thiostrepton stops transcription and translation of plastid genes at 8μM, a concentration which has very little effect on cytosolic protein synthesis [45, 53, 54]. Taken together, these data suggest a plastid-targeted mechanism of antimalarial action, but delayed death has been seen in some studies and not others [37] [36].

Clindamycin, the macrolide antibiotics erythromycin and azithromycin, and tetracycline and its derivitives doxycycline and minocycline, clearly cause a delayed death phenotype in treated parasites. In bacteria, clindamycin, erythromycin and azithromycin inhibit translation by interacting with the peptidyl transferase domain of 23S rRNA and blocking transpeptidation. Tetracyclines bind to the 30S ribosomes and prevent access of aa-tRNA to the acceptor site.

Clindamycin treatment and the delayed death it causes have been well characterized in the related apicomplexan *Toxoplasma gondii*. *T. gondii* parasites treated with clindamycin showed no inhibition of replication or survival in the initial host cell, lysis of the host, extracellular survival or invasion of a new host cell [56]. Parasites eventually ceased replicating in the second generation and died. Although less well characterized in *P. falciparum*, parasites treated with any of these translation inhibitors followed a similar fate. Treated parasites divided normally with all merozoites inheriting an apicoplast, but the parasites in the following generation failed to complete schizogony [34, 37, 40].

Additional evidence that these antibiotics target the plastid was obtained through imaging of *P. falciparum* parasites with fluorescently labeled mitochondria and apicoplasts. These parasites looked normal after 48 hours of drug treatment, but in the second generation, the apicoplast did not branch and a single abnormal, diffusely stained apicoplast persisted [34, 37, 40]. The mitochondria may also be affected late in the second generation, but these effects are more subtle and may be a result of the lack of apicoplast function [37].

In addition to the gross morphological defects in the second cycle, the apicoplasts are apparently also non-functional. Treatment with doxycycline or minocycline caused a specific decrease in transcription of apicoplast genes [40, 53]. For doxycycline, this is clearly demonstrated in Chapter 3 using a microarray-based approach which revealed a decrease in expression of all apicoplast genes with no effect on nuclear or mitochondrial genes [40]. We show that this decrease in expression in the second generation is due to a loss of the apicoplast genome [39, 40]. This specific loss of the apicoplast genome was also seen after treatment with clindamycin, erythromycin and azithromycin. Beginning around 48 hours after treatment, parasites had a reduced plastid to genome ratio which became more dramatic after 72 or 96 hours [39, 51]. Protein import into the apicoplast is also disrupted beginning in the second cycle after treatment with azithromycin tetracycline and doxycycline [37, 40]. Although this is an indirect measure of apicoplast function, it does indicate that the apicoplast is not functioning normally.

Finally, resistance has been selected for clindamycin in *Toxoplasma* and azithromycin in *P. falciparum*, and the mutations presumably responsible for causing resistance have been mapped. For clindamycin, the mutation maps to the large subunit rRNA found on the plastid which corresponds to a well-known mutation causing resistance in *E. coli* [57]. The mutation is present on both rDNA copies, indicating strong positive selection under drug pressure. Resistant parasites are also somewhat cross-resistant to chloramphenicol, azithromycin, spiromycin and lincomycin indicating a similar target for all of them [57-59]. Interestingly, the resistant mutant is also slightly hyper-sensitive to doxycycline.

Two azithromycin resistant *P. falciparum* strains have been selected, and both strains have a point mutation converting a glycine to valine in the plastid encoded ribosomal L4 protein [36]. Similar mutations in L4 have been implicated in macrolide resistance in bacteria. One resistant strain also carried a second mutation in domain I of the large subunit rRNA, but this domain has not been previously associated with macrolide resistance [36]. Both resistant strains were cross-resistant to the closely related erythromycin. Additionally, one strain was also hyper-sensitive to tetracycline, doxycycline, and thiostrepton, although this increased sensitivity could be a result of the large subunit rRNA mutation [36]. As described above, clindamycin resistant *T. gondii*, which have mutations in the large subunit rRNA at a different site, are also cross-resistant to azithromycin [57].

Although there is beginning to be agreement about the target of these antibiotics, it is still unclear why killing the apicoplast causes delayed death. One hypothesis is related to protein produrance. Because most proteins used by the apicoplast are actually encoded in the nucleus, halting apicoplast transcription, translation or DNA replication probably affects a relatively small number of proteins. These proteins may become diluted out as the apicoplast divides normally in the first generation and become too scarce by the second generation. Once the apicoplast begins to experience transcriptional or translational inhibition, it may subsequently fail to import nuclear proteins which leads to a completely nonfunctional apicoplast. Biosynthetic pathways such as fatty-acid, isoprenoid, iron-sulfur cluster and heme synthesis normally carried out in the apicoplast shut down, and the parasite cannot live without these products. Although this is a scenario that makes sense, there is no direct evidence that antibiotics cause this chain of

events, and more work is needed to tease out the effects antibacterials have on *Plasmodium.*

Using *Saccharomyces cerevisiae* as a heterologous system to study the structure-function relationship of the *Plasmodium falciparum* chloroquine resistance transporter

Chloroquine began use as an antimalarial during the Second World War and has been the mainstay of malaria treatment. However, resistance began appearing in the 1960s and spread to sub-Saharan Africa in the late 1970s, which has made this inexpensive, safe and previously effective drug almost completely ineffective.

The primary resistance determinant was identified through a genetic cross between a chloroquine-resistant clone, and a chloroquine-sensitive clone [60]. The gene responsible for resistance was a putative transporter with 10 transmembrane domains named the *Plasmodium falciparum* chloroquine resistance transporter (PfCRT). Several different point mutations in PfCRT have been identified in field isolates and have been shown to cause the resistance phenotype in *P. falciparum in vitro* [61]. Although this gene was identified almost 20 years ago and many studies have investigated its function and relationship to resistance, it is still not completely understood how chloroquine resistance is achieved.

It is generally agreed that PfCRT confers resistance by decreasing the accumulation of chloroquine in the digestive vacuole where it exerts its antimalarial effect [62]. The mechanism behind this decrease in chloroquine accumulation remains unclear, but two hypotheses have been proposed [62]. In the first, chloroquine is pumped

out directly by the resistant allele of PfCRT. In the other, the resistant allele of PfCRT somehow changes the pH of the digestive vacuole, making it less acidic. This in turn would trap less of the weakly basic chloroquine in the digestive vacuole. There is currently ample evidence to support both hypotheses, and more work needs to be done to resolve this mystery.

Regardless of the outcome of this controversy, it is still valuable to determine a structure-function relationship for PfCRT. The critical mutation causing resistance is a lysine to threonine mutation at position 76. However, the context of this mutation is highly variable and there are many other mutations found in various resistant strains. Based on structural predictions, it is predicted that the K76T mutation alters the substrate specificity of PfCRT allowing either the direct efflux of chloroquine out of the digestive vacuole, or the leaking of H+ to change the pH. The function and contribution to resistance of the numerous other mutations is unknown. It is also not clearly understood whether any of these mutations are necessary for resistance to other quinoline based compounds.

Because PfCRT is essential in *P. falciparum* it is necessary to investigate its structure function relationship in a heterologous system. This strategy has been used previously with expression of the *P. falciparum* dihydrofolate reductase (PfDHFR) expressed in *S. cerevisiae* [63]. In that study, the group was able to successfully recapitulate sensitive and resistant phenotypes to known resistance alleles in yeast to both pyremethamine and WR99210. They then used PCR mutagenesis to look for other areas of the protein that caused increased resistance to both drugs when mutated and found three regions of the protein which were clearly involved in resistance.

Several attempts have been made to study PfCRT in heterologous systems [64, 65]. The first study used a recoded PfCRT with modified N and C termini to promote membrane localization [65]. This modified PfCRT was expressed in *S. cerevisiae* and *Pichia pastoris*. Inside out membrane vesicles containing PfCRT where then tested for changes in pH gradient formation. The chloroquine resistant Dd2 allele showed verapamil reversible changes in pH gradient formation when Cl^- was present, while the sensitive HB3 allele showed no change. The Dd2 allele also had an increased release of inorganic phosphate, possibly indicating increased H^+ translocation and ATPase activity. The authors concluded that PfCRT directly or indirectly mediates Cl^- movements to maintain pH in the digestive vacuole. Although this study begins to determine a role for PfCRT in *P. falciparum*, it did not determine a specific mechanism for resistance. Also, the protein was extensively modified, which could impact function.

The second study to use a heterologous system expressed a recoded but otherwise unmodified PfCRT in *Xenopus laevis* [64]. Immunofluorescence was used to show that PfCRT localizes to the membrane, although it may actually be localized to vesicles just below the membrane. The authors then showed that expressed PfCRT causes alkalinization of the cell as well as a depolarized resting potential. It is unclear how these results relate to a physiological role of PfCRT, and this study used only a chloroquine-sensitive allele which offers no insight into a mechanism of resistance.

Chapter 4 describes a heterologous system for expressing recoded PfCRT in *S. cerevisiae*. In this system, we are attempting to determine a structure-function relationship for this protein, similar to the experiment described above for PfDHFR. However, because *S. cerevisiae* is naturally extremely resistant to chloroquine, we have

first focused on sensitizing the system so that small differences between resistant and sensitive alleles can be observed. One way to find a more sensitive readout, is to use microarrays to look for genes with a strong response to chloroquine. Ideally these genes would also have a distinguishable response between strains expressing sensitive and resistant alleles of PfCRT.

We have found a group of genes representing several distinct pathways which respond to chloroquine and appear to show a differential response between strains with sensitive and resistant alleles. These genes fall mainly into a few different pathways involved in mannoprotein and cell wall signaling. Many of the genes in these pathways also cause increased sensitivity to chloroquine when knocked out in yeast. Using engineered promoters with response elements from these pathways driving a selectable marker, we should be able to screen a large number of mutants to test the structure-function relationship in PfCRT.

Once we have a clear idea of what areas of the protein are important for resistance, we can begin to use this system as a platform to screen new 4-amino quinolines. Drugs that can quickly achieve resistance through similar point mutations can be discarded early in the pipeline, so that drugs with a better chance for a long period of succesful clinical use can be chosen.

In summary, this thesis describes three different ways to use DNA microarrays to advance our understanding of *P. falciparum* biology and to study more applicable problems such as mechanisms of drug action and mechanisms of drug resistance.

References

1. Snow RW, Guerra CA, Noor AM, Myint HY, Hay SI: **The global distribution of clinical episodes of Plasmodium falciparum malaria**. *Nature* 2005, **434**(7030):214-217.
2. Yamey G: **Roll Back Malaria: a failing global health campaign**. *Bmj* 2004, **328**(7448):1086-1087.
3. Bozdech Z, Llinas M, Pulliam BL, Wong ED, Zhu J, DeRisi JL: **The transcriptome of the intraerythrocytic developmental cycle of Plasmodium falciparum**. *PLoS Biol* 2003, **1**(1):E5.
4. Le Roch KG, Zhou Y, Blair PL, Grainger M, Moch JK, Haynes JD, De La Vega P, Holder AA, Batalov S, Carucci DJ *et al*: **Discovery of gene function by expression profiling of the malaria parasite life cycle**. *Science* 2003, **301**(5639):1503-1508.
5. Tarun AS, Peng X, Dumpit RF, Ogata Y, Silva-Rivera H, Camargo N, Daly TM, Bergman LW, Kappe SH: **A combined transcriptome and proteome survey of malaria parasite liver stages**. *Proc Natl Acad Sci U S A* 2008, **105**(1):305-310.
6. Young JA, Fivelman QL, Blair PL, de la Vega P, Le Roch KG, Zhou Y, Carucci DJ, Baker DA, Winzeler EA: **The Plasmodium falciparum sexual development transcriptome: a microarray analysis using ontology-based pattern identification**. *Mol Biochem Parasitol* 2005, **143**(1):67-79.
7. Brazas MD, Hancock RE: **Using microarray gene signatures to elucidate mechanisms of antibiotic action and resistance**. *Drug Discov Today* 2005, **10**(18):1245-1252.
8. Hughes TR, Hiley SL, Saltzman AL, Babak T, Blencowe BJ: **Microarray analysis of RNA processing and modification**. *Methods Enzymol* 2006, **410**:300-316.
9. Raghavan A, Bohjanen PR: **Microarray-based analyses of mRNA decay in the regulation of mammalian gene expression**. *Brief Funct Genomic Proteomic* 2004, **3**(2):112-124.
10. Silvestrini F, Bozdech Z, Lanfrancotti A, Di Giulio E, Bultrini E, Picci L, Derisi JL, Pizzi E, Alano P: **Genome-wide identification of genes upregulated at the onset of gametocytogenesis in Plasmodium falciparum**. *Mol Biochem Parasitol* 2005, **143**(1):100-110.
11. Balaji S, Babu MM, Iyer LM, Aravind L: **Discovery of the principal specific transcription factors of Apicomplexa and their implication for the evolution of the AP2-integrase DNA binding domains**. *Nucleic Acids Res* 2005, **33**(13):3994-4006.
12. Coulson RM, Hall N, Ouzounis CA: **Comparative genomics of transcriptional control in the human malaria parasite Plasmodium falciparum**. *Genome Res* 2004, **14**(8):1548-1554.
13. Gunasekera AM, Myrick A, Militello KT, Sims JS, Dong CK, Gierahn T, Le Roch K, Winzeler E, Wirth DF: **Regulatory motifs uncovered among gene**

expression clusters in Plasmodium falciparum. *Mol Biochem Parasitol* 2007, **153**(1):19-30.
14. van Noort V, Huynen MA: **Combinatorial gene regulation in Plasmodium falciparum**. *Trends Genet* 2006, **22**(2):73-78.
15. Young JA, Johnson JR, Benner C, Yan SF, Chen K, Le Roch KG, Zhou Y, Winzeler EA: **In silico discovery of transcription regulatory elements in Plasmodium falciparum**. *BMC Genomics* 2008, **9**:70.
16. Mair GR, Braks JA, Garver LS, Wiegant JC, Hall N, Dirks RW, Khan SM, Dimopoulos G, Janse CJ, Waters AP: **Regulation of sexual development of Plasmodium by translational repression**. *Science* 2006, **313**(5787):667-669.
17. Cheadle C, Fan J, Cho-Chung YS, Werner T, Ray J, Do L, Gorospe M, Becker KG: **Control of gene expression during T cell activation: alternate regulation of mRNA transcription and mRNA stability**. *BMC Genomics* 2005, **6**(1):75.
18. Fan J, Yang X, Wang W, Wood WH, 3rd, Becker KG, Gorospe M: **Global analysis of stress-regulated mRNA turnover by using cDNA arrays**. *Proc Natl Acad Sci U S A* 2002, **99**(16):10611-10616.
19. Meyer S, Temme C, Wahle E: **Messenger RNA turnover in eukaryotes: pathways and enzymes**. *Crit Rev Biochem Mol Biol* 2004, **39**(4):197-216.
20. He F, Li X, Spatrick P, Casillo R, Dong S, Jacobson A: **Genome-wide analysis of mRNAs regulated by the nonsense-mediated and 5' to 3' mRNA decay pathways in yeast**. *Mol Cell* 2003, **12**(6):1439-1452.
21. Houalla R, Devaux F, Fatica A, Kufel J, Barrass D, Torchet C, Tollervey D: **Microarray detection of novel nuclear RNA substrates for the exosome**. *Yeast* 2006, **23**(6):439-454.
22. Cao D, Parker R: **Computational modeling of eukaryotic mRNA turnover**. *Rna* 2001, **7**(9):1192-1212.
23. Garneau NL, Wilusz J, Wilusz CJ: **The highways and byways of mRNA decay**. *Nat Rev Mol Cell Biol* 2007, **8**(2):113-126.
24. Collart MA: **Global control of gene expression in yeast by the Ccr4-Not complex**. *Gene* 2003, **313**:1-16.
25. Dziembowski A, Lorentzen E, Conti E, Seraphin B: **A single subunit, Dis3, is essentially responsible for yeast exosome core activity**. *Nat Struct Mol Biol* 2007, **14**(1):15-22.
26. Liu Q, Greimann JC, Lima CD: **Reconstitution, activities, and structure of the eukaryotic RNA exosome**. *Cell* 2006, **127**(6):1223-1237.
27. Estevez AM, Kempf T, Clayton C: **The exosome of Trypanosoma brucei**. *Embo J* 2001, **20**(14):3831-3839.
28. Estevez AM, Lehner B, Sanderson CM, Ruppert T, Clayton C: **The roles of intersubunit interactions in exosome stability**. *J Biol Chem* 2003, **278**(37):34943-34951.
29. Newbury SF: **Control of mRNA stability in eukaryotes**. *Biochem Soc Trans* 2006, **34**(Pt 1):30-34.
30. Wang Y, Liu CL, Storey JD, Tibshirani RJ, Herschlag D, Brown PO: **Precision and functional specificity in mRNA decay**. *Proc Natl Acad Sci U S A* 2002, **99**(9):5860-5865.

31. Lam LT, Pickeral OK, Peng AC, Rosenwald A, Hurt EM, Giltnane JM, Averett LM, Zhao H, Davis RE, Sathyamoorthy M *et al*: **Genomic-scale measurement of mRNA turnover and the mechanisms of action of the anti-cancer drug flavopiridol**. *Genome Biol* 2001, **2**(10):RESEARCH0041.
32. Garcia-Martinez J, Aranda A, Perez-Ortin JE: **Genomic run-on evaluates transcription rates for all yeast genes and identifies gene regulatory mechanisms**. *Mol Cell* 2004, **15**(2):303-313.
33. Divo AA, Geary TG, Jensen JB: **Oxygen- and time-dependent effects of antibiotics and selected mitochondrial inhibitors on Plasmodium falciparum in culture**. *Antimicrob Agents Chemother* 1985, **27**(1):21-27.
34. Dahl EL, Rosenthal PJ: **Multiple antibiotics exert delayed effects against the Plasmodium falciparum apicoplast**. *Antimicrob Agents Chemother* 2007, **51**(10):3485-3490.
35. Pradines B, Spiegel A, Rogier C, Tall A, Mosnier J, Fusai T, Trape JF, Parzy D: **Antibiotics for prophylaxis of Plasmodium falciparum infections: in vitro activity of doxycycline against Senegalese isolates**. *Am J Trop Med Hyg* 2000, **62**(1):82-85.
36. Sidhu AB, Sun Q, Nkrumah LJ, Dunne MW, Sacchettini JC, Fidock DA: **In vitro efficacy, resistance selection, and structural modeling studies implicate the malarial parasite apicoplast as the target of azithromycin**. *J Biol Chem* 2007, **282**(4):2494-2504.
37. Goodman CD, Su V, McFadden GI: **The effects of anti-bacterials on the malaria parasite Plasmodium falciparum**. *Mol Biochem Parasitol* 2007, **152**(2):181-191.
38. Pradines B, Rogier C, Fusai T, Mosnier J, Daries W, Barret E, Parzy D: **In vitro activities of antibiotics against Plasmodium falciparum are inhibited by iron**. *Antimicrob Agents Chemother* 2001, **45**(6):1746-1750.
39. Ramya TN, Mishra S, Karmodiya K, Surolia N, Surolia A: **Inhibitors of nonhousekeeping functions of the apicoplast defy delayed death in Plasmodium falciparum**. *Antimicrob Agents Chemother* 2007, **51**(1):307-316.
40. Dahl EL, Shock JL, Shenai BR, Gut J, DeRisi JL, Rosenthal PJ: **Tetracyclines specifically target the apicoplast of the malaria parasite Plasmodium falciparum**. *Antimicrob Agents Chemother* 2006, **50**(9):3124-3131.
41. Ralph SA, D'Ombrain MC, McFadden GI: **The apicoplast as an antimalarial drug target**. *Drug Resist Updat* 2001, **4**(3):145-151.
42. Ralph SA, van Dooren GG, Waller RF, Crawford MJ, Fraunholz MJ, Foth BJ, Tonkin CJ, Roos DS, McFadden GI: **Tropical infectious diseases: metabolic maps and functions of the Plasmodium falciparum apicoplast**. *Nat Rev Microbiol* 2004, **2**(3):203-216.
43. Marechal E, Cesbron-Delauw MF: **The apicoplast: a new member of the plastid family**. *Trends Plant Sci* 2001, **6**(5):200-205.
44. Wilson RJ, Denny PW, Preiser PR, Rangachari K, Roberts K, Roy A, Whyte A, Strath M, Moore DJ, Moore PW *et al*: **Complete gene map of the plastid-like DNA of the malaria parasite Plasmodium falciparum**. *J Mol Biol* 1996, **261**(2):155-172.

45. Chaubey S, Kumar A, Singh D, Habib S: **The apicoplast of Plasmodium falciparum is translationally active**. *Mol Microbiol* 2005, **56**(1):81-89.
46. Wilson RJ, Rangachari K, Saldanha JW, Rickman L, Buxton RS, Eccleston JF: **Parasite plastids: maintenance and functions**. *Philos Trans R Soc Lond B Biol Sci* 2003, **358**(1429):155-162; discussion 162-154.
47. Choi SR, Mukherjee P, Avery MA: **The fight against drug-resistant malaria: novel plasmodial targets and antimalarial drugs**. *Curr Med Chem* 2008, **15**(2):161-171.
48. Weissig V, Vetro-Widenhouse TS, Rowe TC: **Topoisomerase II inhibitors induce cleavage of nuclear and 35-kb plastid DNAs in the malarial parasite Plasmodium falciparum**. *DNA Cell Biol* 1997, **16**(12):1483-1492.
49. Williamson DH, Preiser PR, Moore PW, McCready S, Strath M, Wilson RJ: **The plastid DNA of the malaria parasite Plasmodium falciparum is replicated by two mechanisms**. *Mol Microbiol* 2002, **45**(2):533-542.
50. Dar MA, Sharma A, Mondal N, Dhar SK: **Molecular cloning of apicoplast-targeted Plasmodium falciparum DNA gyrase genes: unique intrinsic ATPase activity and ATP-independent dimerization of PfGyrB subunit**. *Eukaryot Cell* 2007, **6**(3):398-412.
51. Fichera ME, Roos DS: **A plastid organelle as a drug target in apicomplexan parasites**. *Nature* 1997, **390**(6658):407-409.
52. Strath M, Scott-Finnigan T, Gardner M, Williamson D, Wilson I: **Antimalarial activity of rifampicin in vitro and in rodent models**. *Trans R Soc Trop Med Hyg* 1993, **87**(2):211-216.
53. Lin Q, Katakura K, Suzuki M: **Inhibition of mitochondrial and plastid activity of Plasmodium falciparum by minocycline**. *FEBS Lett* 2002, **515**(1-3):71-74.
54. McConkey GA, Rogers MJ, McCutchan TF: **Inhibition of Plasmodium falciparum protein synthesis. Targeting the plastid-like organelle with thiostrepton**. *J Biol Chem* 1997, **272**(4):2046-2049.
55. Clough B, Strath M, Preiser P, Denny P, Wilson IR: **Thiostrepton binds to malarial plastid rRNA**. *FEBS Lett* 1997, **406**(1-2):123-125.
56. Fichera ME, Bhopale MK, Roos DS: **In vitro assays elucidate peculiar kinetics of clindamycin action against Toxoplasma gondii**. *Antimicrob Agents Chemother* 1995, **39**(7):1530-1537.
57. Camps M, Arrizabalaga G, Boothroyd J: **An rRNA mutation identifies the apicoplast as the target for clindamycin in Toxoplasma gondii**. *Mol Microbiol* 2002, **43**(5):1309-1318.
58. Pfefferkorn ER, Borotz SE: **Comparison of mutants of Toxoplasma gondii selected for resistance to azithromycin, spiramycin, or clindamycin**. *Antimicrob Agents Chemother* 1994, **38**(1):31-37.
59. Pfefferkorn ER, Nothnagel RF, Borotz SE: **Parasiticidal effect of clindamycin on Toxoplasma gondii grown in cultured cells and selection of a drug-resistant mutant**. *Antimicrob Agents Chemother* 1992, **36**(5):1091-1096.
60. Wellems TE, Panton LJ, Gluzman IY, do Rosario VE, Gwadz RW, Walker-Jonah A, Krogstad DJ: **Chloroquine resistance not linked to mdr-like genes in a Plasmodium falciparum cross**. *Nature* 1990, **345**(6272):253-255.

61. Sidhu AB, Verdier-Pinard D, Fidock DA: **Chloroquine resistance in Plasmodium falciparum malaria parasites conferred by pfcrt mutations**. *Science* 2002, **298**(5591):210-213.
62. Bray PG, Martin RE, Tilley L, Ward SA, Kirk K, Fidock DA: **Defining the role of PfCRT in Plasmodium falciparum chloroquine resistance**. *Mol Microbiol* 2005, **56**(2):323-333.
63. Ferlan JT, Mookherjee S, Okezie IN, Fulgence L, Sibley CH: **Mutagenesis of dihydrofolate reductase from Plasmodium falciparum: analysis in Saccharomyces cerevisiae of triple mutant alleles resistant to pyrimethamine or WR99210**. *Mol Biochem Parasitol* 2001, **113**(1):139-150.
64. Nessler S, Friedrich O, Bakouh N, Fink RH, Sanchez CP, Planelles G, Lanzer M: **Evidence for activation of endogenous transporters in Xenopus laevis oocytes expressing the Plasmodium falciparum chloroquine resistance transporter, PfCRT**. *J Biol Chem* 2004, **279**(38):39438-39446.
65. Zhang H, Howard EM, Roepe PD: **Analysis of the antimalarial drug resistance protein Pfcrt expressed in yeast**. *J Biol Chem* 2002, **277**(51):49767-49775.

Chapter 2: Whole genome analysis of mRNA decay in *Plasmodium falciparum* reveals a global lengthening of mRNA half-life during the intraerythrocytic development cycle

This chapter is a reprint from the following reference:

Shock, J.L., Fischer, K.F. and DeRisi, J.L. (2007) Whole genome analysis of mRNA decay in *Plasmodium falciparum* reveals a global lengthening of mRNA half-life during the intraerythrocytic development cycle. Genome Biology 8(7):R134.

Author contributions:

Jennifer Shock performed the nuclear run-on experiments described in figure 1, the microarray experiments described in figures 2, 3, 4 and 6, the northern blot experiments described in figure 5, and the data analysis described in tables 1 and 2 and figue 6. Kael Fischer wrote several programs to computationally determine the best decay fit for each gene and to generate the decay profile images for each gene shown in figure 3. Joseph DeRisi supervised the research.

Joseph L. DeRisi, thesis advisor

Abstract

Background

The rate of mRNA decay is an essential element of post-transcriptional regulation in all organisms. Previously, studies in several organisms found that the specific half-life of each mRNA is precisely related to its physiological role, and plays an important role in determining levels of gene expression.

Results

We have used a genome wide approach to characterize mRNA decay in *Plasmodium falciparum*. We found that globally, rates of mRNA decay increase dramatically during the asexual intraerythrocytic developmental cycle. During the ring stage of the cycle, the average mRNA half-life was 9.5 minutes, yet this was extended to an average of 65 minutes during the late schizont stage of development. Thus a major determinant of mRNA decay rate appears to be linked to the stage of intraerythrocytic development. Furthermore, we have found specific variations in decay patterns superimposed upon the dominant trend of progressive half-life lengthening. These variations in decay pattern were frequently enriched for genes with specific cellular functions or processes.

Conclusions

Elucidation of *Plasmodium* mRNA decay rates provides a key element for deciphering mechanisms of genetic control in this parasite, by complementing and extending previous mRNA abundance studies. Our results indicate that progressive stage-dependent decreases in mRNA decay rate function are a major determinant of mRNA accumulation

during the schizont stage of intraerythrocytic development. This type of genome wide change in mRNA decay rate has not been observed in any other organism to date, and indicates that post-transcriptional regulation may be the dominant mechanism of gene regulation in *P. falciparum.*

Background

Plasmodium falciparum is the most deadly of the four *Plasmodia* species that cause human malaria, and is responsible for more than 500 million clinical episodes and 1 million deaths per year [1]. Because of increasing worldwide resistance to the most affordable and accessible antimalarial drugs, this number is expected to increase in the near future. In fact, deaths from malaria have increased over the past six years, despite a global health initiative designed to halve the burden of malaria by 2010 [2]. A more thorough understanding of the molecular biology of *P. falciparum* is an important step toward the identification of new drug and vaccine targets.

The *P. falciparum* 48-hour asexual intraerythrocytic development cycle (IDC) is characterized by the progression of the parasite through several distinct morphological stages: ring, trophozoite and schizont. Each cycle begins with invasion of an erythrocyte by a merozoite, followed by the remodeling of the host cell in the ring stage. The parasite then progresses into the trophozoite stage, where it continues to grow and is highly metabolically active. Finally, in the schizont stage, the parasite prepares for the next round of invasion by replicating its DNA and packaging merozoites.

The completion of the *P. falciparum* genome sequence represents a milestone toward our understanding of this parasite and has subsequently enabled numerous genomic and proteomic projects [3]. In previously published work, our laboratory has exhaustively profiled genome-wide mRNA abundance at a one hour time resolution throughout the IDC for three separate strains of *P. falciparum* [4, 5]. Analysis of the IDC transcriptome revealed a cascade of highly periodic gene expression, unlike that seen in

any other organism studied to date. Little is known about how this unique pattern of regulation is established or maintained.

The relative abundance of mRNA, as measured by conventional expression profiling, is a result of the rate at which each message is produced, offset by the rate at which each message is degraded. When compared to organisms with similar genome sizes, the *P. falciparum* genome appears to encode only about a third the number of proteins associated with transcription [6]. Given this apparent lack of a full transcriptional control repertoire, unexpected post-transcriptional mechanisms, including mRNA decay, may contribute significantly to gene regulation.

Currently, there is very little known about the components of mRNA decay in *P. falciparum*, and few of the proteins involved in mRNA decay are annotated. Using the protein sequence of known decay factors from humans and *S. cerevisiae*, we identified putative orthologs to decay components (Table 1).

Studies in mammals and the budding yeast *Saccharomyces cerevisiae* have identified two major pathways for the degradation of mRNA, both of which are deadenylation dependent: 5' to 3' decay and 3' to 5' decay [7]. Both pathways of mRNA decay in mammals and *S. cerevisiae* begin with deadenylation, which is carried out by 3' exonucleases specific for the poly(A) tail, and is thought to be the rate-limiting step of mRNA decay [8]. The major deadenylase in mammalian cells is PARN, an RNase D homolog that is conserved in many eukaryotes. In *S. cerevisiae*, deadenylation is carried out by two complexes: Pan2p/Pan3p and Ccr4p/Pop2p. The Ccr4p/Pop2p complex is the dominant deadenylase in yeast, and is part of a much larger complex called the Ccr4/Not complex, which also has roles in transcription initiation and elongation and protein

modification, suggesting the possibility that these processes are coordinately regulated [9, 10].

Following deadenylation, transcripts can be degraded via one of two distinct pathways. In 5' to 3' decay, Dcp1p and Dcp2p decap the transcript leaving the 5' end vulnerable to decay. There are also a number of enhancers and regulators of decapping including Edc1p-3p, the Lsm complex and the DEAD box helicase Dhh1p. After decapping, subsequent degradation of the transcript proceeds through Xrn1p, the major 5' to 3' exonuclease. Eukaryotes also possess a related exonuclease called Rat1p, which is thought to function mainly in the nucleus.

In contrast to 5' to 3' decay, in 3' to 5' decay, transcripts are degraded by the exosome following deadenylation. The exosome is a complex containing 10 essential proteins, nine of which have a 3' to 5' exonuclease domain. An eleventh component, Rrp6p, is associated with the exosome only in the nucleus and is not essential. Also associated with the exosome are two helicases: Ski2p and Mtr4p. Lastly, the free cap generated by 3' to 5' decay is hydrolyzed by scavenger protein, Dcs1p.

Orthologs for Rrp43p, Rrp46p and Mtr3p have not yet been identified in *P. falciparum*. Interestingly, these same proteins were difficult to identify in *Trypanosoma brucei* as well, but were eventually identified through association with other exosome components [11, 12]. Unfortunately, using the newly identified *T. brucei* components does not identify any additional exosome components in *P. falciparum*.

The numerous factors that constitute the decay machinery regulate the degradation rates of every cellular transcript. The complexity of the system allows for many possible avenues of regulation, including interactions between specific RNA

binding proteins and motifs in the 3' UTRs of transcripts, developmental regulation of decay components, and localization of factors or RNAs to specific compartments in the cell such as P bodies [13]. Any of these methods of regulation are possible in *P. falciparum*. In particular, developmental regulation of decay components is an attractive model considering that many of the putative decay components in *P. falciparum* are transcriptionally regulated during the IDC, with peak expression during the ring to early trophozoite stages[4].

In mammals and yeast, the specific half-life of each mRNA is precisely related to its physiological role and in many cases can be altered in response to different stimuli or developmental conditions [13-16]. For example, it was found in yeast that core metabolic genes such as those encoding glycolytic enzymes produce mRNAs with very long half-lives, yet genes encoding components of the mating type signaling pathway produce mRNAs with very short half-lives.

Thus far, decay rates have not been determined for any *P. falciparum* transcripts, nor have any of the mRNA decay components been genetically or biochemically characterized. Given that mRNA decay is an integral component of gene expression regulation, we conducted a genome-wide study of mRNA decay in *P. falciparum* using a microarray-based approach to measure mRNA half-life as a function of the IDC. Interestingly, we found that a major determinant of mRNA decay rate appears to be tightly linked to intraerythrocytic developmental cycle, and to a lesser extent, the functional category of the mRNAs themselves. Decay rates in the early hours post invasion are rapid and tightly distributed, yet by the end of the cycle, global decay rates decrease considerably, causing a lengthening of half-lives. An analogous genome-wide

change in mRNA decay rate during a development cycle has not been observed in any other organism to date.

Results

Overview of the data

To explore the role of mRNA decay during the IDC of *P. falciparum*, we used microarrays to determine decay rates on a genome-wide scale at four distinct stages. Using aliquots from a single synchronized culture of 3D7 strain parasites (sequenced strain), transcription was inhibited and total RNA was harvested for microarray hybridization. Transcriptional shut off was achieved by addition of actinomycin D (actD), which is known to intercalate into DNA and inhibit DNA dependant RNA polymerases [17]. Actinomycin D has also been shown previously to strongly inhibit *P. falciparum* transcription in a dose dependent manner, with little or no RNA synthesis seen at higher drug concentrations [18]. We have further confirmed transcription inhibition in our own experimental conditions through nuclear run-on experiments using synchronous cultures in the ring and late schizont stages and we note that the degree of relative transcriptional inhibition was approximately equal between ring and schizont stage parasites (Figure 1). While some residual labeling of nuclear run-on RNA was observed after treatment with actD in both stages, any remaining transcriptional activity over the course of the experiment is not anticipated to affect the determination of the decay rate (Materials and Methods). While it remains a formal possibility that treatment with actD could alter the activity of decay processes through indirect or secondary effects, no such effects have been reported in other organisms to our knowledge.

For each of the four decay time-courses, an initial sample was harvested immediately before addition of drug, followed by eight more samples at intervals from 0 to 240 minutes (Figure 2). Each sample was mixed with a reference pool and applied to a 70mer DNA oligonucleotide microarray in a standard two-color competitive hybridization [19]. This experiment was repeated every 12 hours throughout the IDC starting in the ring stage. A Pearson correlation was used to compare the zero minute (untreated cells) results at each of the four stages to the previously characterized 48-hour transcriptome of the HB3 strain [4]. The highest correlations between the decay experiments and the transcriptome data were at 10, 20, 31 and 44 hours post-invasion, corresponding to the ring, trophozoite, schizont and late schizont stages, respectively (r = 0.79, 0.80, 0.67, and 0.73 respectively). The hour of peak correlation for subsequent time points in each of the four separate time courses were unchanged although the actual correlation value progressively decreased, consistent with global transcriptional shutoff at each stage. Using RNA samples from the same experiment, each microarray hybridization was performed at least twice, and in most cases, three times.

The data from each series of microarrays were fit to an exponential decay curve using nonlinear least squares fit, and the half-life was calculated for the transcript hybridized to each oligo at each of the four stages analyzed (Dataset 1). Figure 3 shows arbitrarily chosen examples of decay curves for four individual transcripts, each at one of the four stages. A set of 6,225 oligos (representing 4,783 genes) passed our quality control filters and had a fit decay curve for at least one stage (Materials and Methods). Of these, 3,903 oligos (representing 2,744 genes) had a calculated half-life for all four

stages. The decay curves for these genes are available at http://malaria.ucsf.edu. Those oligos that did not pass the quality control filters are listed in Dataset 2.

Calculated half-lives ranged from one minute to longer than 138 minutes, which was the maximum half-life that could be reliably fit given that each time-course was terminated at 240 minutes after addition of actD. As previously noted, we cannot rule out low levels of ongoing transcription after the addition of drug, however an ongoing zero-order process would not effect our fitted half-lives. (Materials and Methods). Because many genes are represented by more than one oligo, it is possible to use this information to internally corroborate the microarray measurement and calculation of half-lives. In general, half-lives for oligos within a single ORF agreed well (Table 2). For example the average standard deviation for half-lives in the ring stage was 9.9 minutes, while the average standard deviation for half-lives of oligos within a single ORF in the ring stage was 4.6 minutes. Depending on the stage, 13 to 17% of genes which have more than one oligo had poor intragenic correlations, with greater than two standard deviation difference for oligos within a single ORF. There may be underlying technical or biological explanations for discrepancies in these genes. Since the vast majority of annotated genes in the *P. falciparum* genome exist only as gene models without experimental validation, oligos thought to be common to a given gene may in fact be hybridizing to distinct transcripts. Furthermore, alternative splicing of transcripts and bias in the directionality of decay may also result in poor intragenic correlations.

All mRNA half-lives increase during the IDC

Figure 4 shows the distributions of mRNA half-lives for each stage. Beginning with ring stage parasites and ending with late schizonts, we observed a striking increase in half-life for essentially all transcripts measured as a function of the IDC. In the ring stage, the mean half-life was 9.5 minutes and the distribution of half-lives was very narrow with a standard deviation of only 9.9 minutes (Table 2). In the later stages, the average half-life progressively lengthened and the distribution progressively widened. By the late schizont stage, the mean half-life for all transcripts had increased more than 6-fold (65.4 minutes) and the standard deviation had increased by 4-fold (42.6 minutes). While the scope of mRNA decay studies have been limited to model systems or mammalian cells, this progressive and dramatic shift in global mRNA decay rates as a function of developmental cell cycle has not been previously observed in any other organism to date.

We compared half-life to ORF length and relative transcript abundance, and as in yeast and mammalian cells, no strong correlation was found, indicating that mRNA decay in *P. falciparum* is most likely a regulated process rather than a simple, basal degradation of all transcripts [14, 20]. Although there exists a global trend in decay rate change common to all genes, we sought to determine whether individual patterns of rate change correlated with the corresponding profile of steady-state abundance, measured previously[5]. We found no significant correlation between the transcriptome phase of each gene (roughly, when the peak of expression occurs during the IDC) and it's pattern of half-life change (data not shown).

The half-lives for PFB0760w and PF13_0116, two genes with large stage-dependent changes in decay rate, were confirmed by Northern blot analysis for the ring

and late schizont stages (Figure 5). Half-lives calculated by Northern blot were in good agreement with those calculated by microarray. The half-lives for PFB0760w in the ring and schizont stages were calculated to be 6.7 and 54.1 minutes, respectively, by microarray analysis and 3.7 and 35.6 minutes by Northern analysis. For PF13_0116 the half-life calculated by microarray was 5.4 minutes in the ring stage compared to 8.8 minutes calculated by Northern blot. The half-life for the late schizont stage was greater than 138 minutes when calculated with either method.

It has previously been shown that transcripts from *Plasmodium* species can have multiple polyadenylation sites [21, 22]. While no obvious difference in transcript length was evident at the resolution of the Northern blots, we specifically investigated the possibility that changes in UTR length were concomitant with changes in decay rate. We analyzed the 5' UTRs of PF13_0116 and PFB0760w (the same genes used in the Northern blot analysis) using rapid amplification of cDNA ends (RACE) for the ring and late schizont stages. The lengths of the 5' UTRs for these two genes were measured to be 185 bp and 836 bp, respectively. For both genes in both stages, there was no change in the RACE products and at least for these representative genes, changes in site selection for transcription initiation were not evident and are therefore not linked to the observed lengthening of half-life during the IDC. We attempted 3' RACE on these genes, but because of the extreme A/T richness of *P. falciparum* UTRs, we cannot be certain that the UTRS were accurately measured. Thus a change in transcription termination or polyadenylation site could be linked to the lengthening of half-lives.

Decay rate and gene function

In yeast and mammalian cells there is a relationship between decay rate and gene function [14-16]. In particular, transcripts for proteins that function in the same pathway or process generally have similar decay rates. Because the rate of decay for most *P. falciparum* transcripts changes during the IDC, it is inappropriate to determine a single half-life for each transcript. However, we wished to investigate the possibility that the pattern of decay rate change could be used to partition the dataset into distinct groups. We used k-means clustering of the half-lives for all four stages into ten groups followed by GO term analysis (GoStat) to detect enrichment of gene function or process (Figure 6) [23]. We tested several different numbers of groups, and dividing the data into ten groups best matches the natural structure of the data, and gives the lowest p-values for the GO term analysis. To ensure that the clusters were not an artifact of the cyclical nature of steady-state expression *in P. falciparum*, we compared the distributions of transcriptome phases, which represent the stage of peak expression, for each group and found no significant correlation (data not shown).

Although all ten groups have a pattern of increasing half-lives in which the late stage half-lives are longer than the ring stage half-lives, there are differences in the pattern and scale of half-life increase. These differences are illustrated in the plots showing the average half-lives for each group and the increase in half-life from the ring to late schizont stage in Figure 6. The decay rate progressively decreases in each stage for six of the ten groups. Of the four remaining groups, groups 8 and 9 have trophozoite stage half-lives that are shorter than their ring stage half-lives, group 5 has late stage half-

lives shorter than its schizont stage half-lives, and group 10 has a unique decay pattern with transcripts being most stable in the trophozoite stage.

Nine of the ten groups are associated with significantly over-represented GO terms and the complete list of significant terms and corresponding p-values can be found in Dataset 3. A range of GO terms were represented amongst the different groups, and in general over-represented terms in the same group were involved in similar processes. Listed below are the four groups with the most significant GO terms (lowest p-value).

Transcripts clustered in group 1 display a relatively stable pattern of decay, with an increase in half-life of 31 minutes between the ring and late schizont stages, compared with a genome-wide average increase of 56 minutes. Group 1 also has the longest average half-life in the ring stage. This group has several highly over-represented terms including ribosome, ribonucleoprotein complex, cytoskeleton organization and biogenesis and mitochondrion. Given that all these terms represent proteins involved in processes that are active throughout the life cycle, it is not surprising to see them in the cluster with the lowest half-life variability across the IDC. While group 4 also has over-represented GO terms for processes needed throughout the life-cycle, the genes in this group have a pattern of decay which most closely matches the average half-life increase seen across the genome. Terms for the generation of metabolites and energy, cellular catabolism and TCA cycle metabolism were all found in this group. Wang and colleagues found that in yeast, genes involved in energy metabolism had similar, very long half-lives [14]. Instead, our data suggest the decay rate in *P. falciparum* might be matched to the energy requirements of the growing cell. Group 5 also has a relatively stable pattern of decay, but does not have longer than average half-lives in the ring stage.

This group is enriched in terms involved in RNA processing including nucleolus, rRNA metabolism and nuclear mRNA splicing, via spliceosome. Group 10 has the most unusual profile with a short average half-life in the ring and schizont stages and a long average half-life in the trophozoite and late schizont stages. This group has terms involved in pathogenesis overrepresented, such as host and antigenic variation.

In a separate analysis, we were able to find over-representation for two sample groups that could be easily annotated by hand using the lexical analysis tool, LACK [24]. Plastid encoded genes and tRNAs, which both lack associated GO terms were over-represented in group 7 (p-value < 3.25×10^{-3} and 4.50×10^{-5}, respectively).

Discussion

In this study, we have shown that the overall rates of decay change during the developmental cycle, beginning with relatively short half-lives in the ring stage and ultimately ending with dramatically longer half-lives in the schizont stage. The abundance of any given mRNA species is the result of transcriptional production offset by the rate of degradation. Thus, a change in transcriptional output without a corresponding change in abundance implies a necessary alteration in the rate of degradation. It has been noted previously that the quantity of mRNA that can be isolated per infected erythrocyte increases dramatically over the course of the IDC [25]. There is also evidence through previously published radioisotope pulse labeling experiments and our own unpublished observations, that transcription increases steadily from invasion until around 36 hours and then drops off in late stage parasites [26, 27]. Therefore, the

observed mRNA accumulation post-schizogony appears to be largely a function of enhanced mRNA stability rather than increasing levels of transcription.

This global stabilization may be a mechanism to regulate gene expression in the late stage parasites, when the process of packaging multiple nuclei into developing merozoites may complicate coordinate regulation of transcription. Stabilized mRNA may also be important for the merozoite, and represent a carefully regulated "starting package" which would allow rapid activation of the IDC following the next round of invasion. Furthermore, the data are consistent with a process by which the low level transcriptional accumulation in early stage parasite development features rapid mRNA turnover, perhaps indicative of the dynamic remodeling process that immediately follows invasion. Future experiments using a pulse-chase system, such as was developed for *Toxoplasma gondii* to measure newly synthesized mRNA and its degradation, could also help elucidate whether this model is correct [28].

The mechanism for the genome-wide increase in mRNA half-lives remains unclear. Similar to yeast and mammalian cells, the rate of decay could not be correlated to transcript length, abundance or transcriptome phase [14, 20].

A straightforward mechanism that could explain the global lengthening of half-lives would include the developmental regulation of the decay components themselves. Indeed, all of the decay components measured by our previous transcriptome profiling efforts exhibit clear patterns of phase specific expression with most profiles indicating peak mRNA abundance in rings and trophozoites [4]. While the mRNA abundance profiles of the decay components are consistent with a model in which the most rapid turnover of mRNA occurs early in the intraerythrocytic developmental cycle, the actual

protein expression profiles of these components remain to be measured. Furthermore, the expression of the proteins themselves may not be coordinated with their activation, thus the actual biochemical activities must also be assessed. For example, a progressive decrease in deadenylation, decapping or exonuclease activity could account for the observed lengthening of half-lives independent of when the proteins are produced. Given the current data, it remains an open question as to whether the observed increases in mRNA half-life are a direct result of limiting quantities of critical decay components or whether additional regulatory factors or physical sequestration limit entry of mRNAs into the decay pathway.

Numerous studies in other organisms have shown that sequence elements in the 3' UTR are important in determining decay rate for many genes [10]. The extreme A/T richness of the *P. falciparum* genome, combined with a lack of functionally characterized UTRs, has made identification of putative decay motifs, which are also generally A/T rich, challenging. However, Coulson et al. found proteins with sequence similarity to RNA binding proteins, in particular the CCCH-type zinc finger proteins involved in regulating mRNA stability, over-represented in *P. falciparum* [6].

In addition to the global change in decay rate, we have also shown that genes grouped by their pattern of decay show significant enrichment of GO terms, suggesting that genes functioning in the same pathway or process have similar decay rates over the life-cycle. This type of coherence in mRNA decay rates for functional groups has also been observed in yeast and mammals [14, 16], and at least two separate factors, RNA polymerase II subunit Rpb4p and Pub1p, have been linked to differential decay of mRNAs encoding protein biogenesis components [29, 30]. In their study of changes in

transcription rate and decay rate during the shift from glucose to galactose in yeast, Garcia-Martinez and colleagues identified several GO categories that have coordinately regulated decay patterns [16]. Interestingly, many of these categories are the same as those identified in this study including ribosomal proteins, proteins involved in energy metabolism and proteins involved in rRNA processing. These authors also measured a general increase in mRNA stability during the shift from glucose to galactose. An analogous mechanism may be responsible for the observed increase in mRNA stability during the *P. falciparum* developmental cycle.

Conclusions

In this study, we have measured the mRNA decay rate in *P. falciparum* for over 4,000 genes during the 48-hour intraerythrocytic life cycle. The characterization of mRNA decay rates on a genome-wide scale during the *P. falciparum* IDC offers insights into the unique biology of the malaria parasite and the unique manner in which gene expression is regulated throughout the intraerythrocytic developmental cycle. This study provides a foundation for continued investigations into the molecular mechanism of *Plasmodium* mRNA decay, and its role in parasite development.

Materials and Methods

Cell culture

P. falciparum parasite cells (3D7) were cultured as described previously [19]. Cells were synchronized by two consecutive sorbitol treatments during two consecutive cell cycles (a total of four treatments) and the mRNA decay experiments were conducted

at 12 hour intervals starting in the ring stage (10-12 h post-invasion). To stop transcription, actinomycin D (Amersham) was added at 20 μg/mL, and samples were collected 0, 5, 10 15, 30, 60, 120 and 240 minutes later. For each mRNA decay experiment, a sample was also taken directly before addition of drug. The cells were harvested by centrifugation at 1,500 x *g* for 5 minutes, washed in PBS, and pelleted at 1,500 *g* for 5 min. Cell pellets were rapidly frozen in liquid nitrogen and stored at -80°C.

RNA preparation and microarray hybridization

Total RNA was prepared directly from the frozen pellets of parasitized erythrocytes, where approximately 1 ml of cell pellet was lysed in 10 ml Trizol (GIBCO). For the hybridization experiments, 8 μg total RNA was used for amino-allyl cDNA synthesis as previously described [19]. A pool of amino-allyl labeled cDNAs representing stages throughout the IDC was assembled and used as a reference. For DNA microarray hybridization, the pool cDNA was always coupled to Cy3 dye as reference, while cDNA from an individual time point was coupled to Cy5 dye.

The DNA microarray used in this study contains 8182 70-mer oligos. Of these 6652 are unique and map to an annotated ORF as listed in PlasmoDB release 4.4. DNA microarrays were printed and post-processed as described [19].

For the trophozoite, schizont and late schizont decay experiments, the individual time points were hybridized in triplicate. For the ring decay experiment, the time points were hybridized in duplicate due to limiting quantities of RNA. In all cases, all time points for a single replicate were hybridized on the same day and included two replicates of the sample collected before addition of actinomycin D.

DNA microarrays were scanned using an Axon 4000B scanner and images analyzed using Axon GenePix software (Molecular Devices, Union City, CA, USA). Microarray data were stored using NOMAD database software (https://ucsf-nomad.sourceforge.net).

For normalization among time points, an internal control was prepared with a pool of *in vitro*-transcribed *Saccharomyces cerevisiae* RNAs. Oligos Y_IBX1991, Y_ICX1881, Y_IFX1541 and Y_IHX3161 (http://derisilab.ucsf.edu/falciparum), representing four intergenic *S. cerevisiae* sequences, were printed 16 times each onto the *P. falciparum* DNA microarrays. RNA transcripts of each of these *S. cerevisiae* DNAs were prepared *in vitro* and pooled. This internal control mix was added to each total RNA sample analyzed in the decay time course, as well as to the total RNA used as pool, at a final concentration of 1 ng of each *S. cerevisiae* RNA per 8 μg of total RNA.

Data Analysis

Decay rates for every transcript for which decay was observed were determined by fitting all observations with a three parameter first order decay model, $A=(A0-B)e^{-\ln(0.5)/t_{1/2}*t}+B$, using the Levenberg-Marquardt algorithm implemented in MINPACK [31]. Using this model, fits of $t_{1/2}$ are insensitive to zero order kinetic contributions, such as continued low levels of transcription. Formally, a zero order contribution to a first order process affects only the final steady state ratio, B in our model, and has no impact on the decay constant or half-life. To ensure that contributions from residual transcription were minimized, all measurements for times under 10 minutes were excluded from the analysis if no decay had been observed for the transcript in question.

All arrays were normalized using the average median intensities of the *in vitro* transcribed *S. cerevisiae* RNA internal controls. The ratio of median intensities for unflagged spots with a median intensity of greater than 300 in either channel was used for further analysis. Several quality control checks were employed before any fits were included in downstream analysis as summarized in Dataset 2. Each decay profile had to pass two sets of filters. First, before any fitting was performed, a set of raw data filters (Group A, Dataset 2) was applied: The profile had to include measurements from at least 8 data points, the observed amplitude had to be at least 0.1, the first time point not later than 10 minutes and the last observation not earlier than 60 minutes. Second, the decay profiles which passed all the Group A tests were fit to the decay model. Fits with systematic residuals were eliminated by filtering out fits in several classes (Group B, Dataset 2). Each fit had to have an amplitude (A_0-B) of at least 0.1 but not more than 10.0, with B between –1.0 and A_0 , and the fit half-life had to be > 1 minute. When < 70% of the fit amplitude was experimentally observed over the time course, we report the half-life as >138 minutes.

Oligos that were excluded from the final analysis are listed for each stage in Dataset 2. Values for each model parameter, initial ratio (A_0), final ratio (B) and half-life ($t_{1/2}$) as well as the asymptotic standard errors for all fits that satisfy those criteria are given in Dataset 1.

K-means clusters were generated using log-transformed half-lives for each gene in each stage. For genes with more than one oligo, the half-lives were averaged if the standard deviation was less than the average standard deviation for all genes with multiple oligos in that stage. The clustering was done only on genes with data present for

at least 3 out of the 4 stages. *K*-means clusters were generated using uncentered mean correlation in Cluster 3.0 and visualized using Java Treeview [32]. Gene Ontology analysis was done using the GoStat tool with the following parameters: minimal length of considered GO paths = 5, maximal p-value = 0.01, cluster GOs = -1, correct for multiple testing = none.

Nuclear run-on analysis

Synchronous cultures in either the ring or late schizont stage were treated with 20μg/mL actinomycin D. Time points were then taken at 0, 7.5 and 15 minutes after addition of drug. Each sample was pelleted and washed once with 1 X PBS before lysis with 1 volume 0.2% saponin. Lysed parasites were washed twice in 1 X PBS and resuspended in 1.5 mL buffer A (20 mM PIPES, 15 mM NaCl, 60 mM KCl, 14 mM 2-mercaptoethanol, 0.5 mM EGTA 4 mM EDTA, 0.5 mM spermidine, 0.125 mM PMSF). The parasites were transferred to a Dounce homogenizer with a type B pestle. 100 μL 10% NP-40 was added and 10 strokes were applied. Nuclei were pelleted by centrifugation for 3 min at 6,000 x *g*, washed in buffer A and pelleted again. Each sample was resuspended in 200 μL buffer B (50 mM HEPES pH 7.9, 50 mM NaCl, 10 mM $MgCl_2$ 1.2 mM DTT, 1 mM GTP, 1 mM CTP, 4 mM ATP, 20% glycerol, 25 U/mL RNasin). 0.5 μM [α-^{32}P]UTP (3000 Ci/mmol) was added to all samples and transcription was allowed to proceed at 37° for 30 minutes. RNA was isolated using Trizol as per the manufacturers instructions. The RNA was hybridized to a dot blot spotted with 500 ng total cDNA in Rapid Hyb buffer (Amersham) at 55° C and washed according to the manufacturers instructions. Spot intensity was measured using a PhosphorImager.

Rapid amplification of cDNA ends (RACE)

5' RACE was done using the First Choice RLM-RACE kit (Ambion) according to the manufacturers instructions. Nested PCR was used and the following primers were used with the primers provided with the kit: 5' TGATTTTACGCTTAAACCAGAGG 3' for the PFB0760w 5' RACE outer primer, 5' CTCTTGTTACTATTATTATTTTGCCCCTCA 3' for the PFB0760w 5' RACE inner primer, 5' TGACCAAAAAGATTTTACTGAA 3' for the PF13_0116 5' RACE outer primer, 5' AAAACTTTCCAAACTTTCACAA 3' for the PF13_0116 5' RACE inner primer. Herculase (Stratagene) was used for all PCRs using the following cycling conditions: 3 min at 94° followed by 35 rounds of 94° for 30 sec, 55° for 30 sec, 60° for 1 min. All PCR products were confirmed by sequencing.

Northern analysis

Northern blots were performed as described [33]. 10 μg of total RNA was used for each sample. The probes were generated using the following PCR primers: 5' CCAAAGGAGGAGACATCCAA 3' and 5' GGGAAACACAATCGCTGAAT 3' for PFB0760w and 5' AGAATGCTTTCCCACGACAC 3' and 5' TGAATCGTTAAAAGACGGATGA 3' for PF13_0116. The PCR products were labeled with [α-^{32}P]dATP using the DECAprime™ II kit (Ambion). The RNA used for the Northerns was the same as that used for the cDNA synthesis.

List of abbreviations

IDC-intraerythrocytic development cycle

actD-actinomycin D

RACE-rapid amplification of cDNA ends

UTR-untranslated region

GO-gene ontology

Acknowledgements

We would like to thank members of the DeRisi lab for helpful advice. We would also like to thank Teresa Shock, Megan Bergkessel, Brad Zuchero, Julie Hollien, Manuel Llinás and Ashwini Jambhekar for helpful discussion and critical comments on the manuscript. This work and JLS were supported by a grant from the National Institute of Allergy and Infectious Disease (U01 AI53862), the Packard Foundation, and the Howard Hughes Medical Institute (HHMI). JDR is supported by HHMI. KFF is supported by a grant from the Doris Duke Foundation.

References

1. Snow RW, Guerra CA, Noor AM, Myint HY, Hay SI: **The global distribution of clinical episodes of Plasmodium falciparum malaria**. *Nature* 2005, **434**(7030):214-217.
2. Yamey G: **Roll Back Malaria: a failing global health campaign**. *Bmj* 2004, **328**(7448):1086-1087.
3. Kooij TW, Janse CJ, Waters AP: **Plasmodium post-genomics: better the bug you know?** *Nat Rev Microbiol* 2006.
4. Bozdech Z, Llinas M, Pulliam BL, Wong ED, Zhu J, DeRisi JL: **The transcriptome of the intraerythrocytic developmental cycle of Plasmodium falciparum**. *PLoS Biol* 2003, **1**(1):E5.
5. Llinas M, Bozdech Z, Wong ED, Adai AT, DeRisi JL: **Comparative whole genome transcriptome analysis of three Plasmodium falciparum strains**. *Nucleic Acids Res* 2006, **34**(4):1166-1173.
6. Coulson RM, Hall N, Ouzounis CA: **Comparative genomics of transcriptional control in the human malaria parasite Plasmodium falciparum**. *Genome Res* 2004, **14**(8):1548-1554.
7. Garneau NL, Wilusz J, Wilusz CJ: **The highways and byways of mRNA decay**. *Nat Rev Mol Cell Biol* 2007, **8**(2):113-126.
8. Cao D, Parker R: **Computational modeling of eukaryotic mRNA turnover**. *Rna* 2001, **7**(9):1192-1212.
9. Collart MA: **Global control of gene expression in yeast by the Ccr4-Not complex**. *Gene* 2003, **313**:1-16.
10. Meyer S, Temme C, Wahle E: **Messenger RNA turnover in eukaryotes: pathways and enzymes**. *Crit Rev Biochem Mol Biol* 2004, **39**(4):197-216.
11. Estevez AM, Kempf T, Clayton C: **The exosome of Trypanosoma brucei**. *Embo J* 2001, **20**(14):3831-3839.
12. Estevez AM, Lehner B, Sanderson CM, Ruppert T, Clayton C: **The roles of intersubunit interactions in exosome stability**. *J Biol Chem* 2003, **278**(37):34943-34951.
13. Newbury SF: **Control of mRNA stability in eukaryotes**. *Biochem Soc Trans* 2006, **34**(Pt 1):30-34.
14. Wang Y, Liu CL, Storey JD, Tibshirani RJ, Herschlag D, Brown PO: **Precision and functional specificity in mRNA decay**. *Proc Natl Acad Sci U S A* 2002, **99**(9):5860-5865.
15. Lam LT, Pickeral OK, Peng AC, Rosenwald A, Hurt EM, Giltnane JM, Averett LM, Zhao H, Davis RE, Sathyamoorthy M *et al*: **Genomic-scale measurement of mRNA turnover and the mechanisms of action of the anti-cancer drug flavopiridol**. *Genome Biol* 2001, **2**(10):RESEARCH0041.
16. Garcia-Martinez J, Aranda A, Perez-Ortin JE: **Genomic run-on evaluates transcription rates for all yeast genes and identifies gene regulatory mechanisms**. *Mol Cell* 2004, **15**(2):303-313.
17. Reich E, Franklin RM, Shatkin AJ, Tatumel: **Action of actinomycin D on animal cells and viruses**. *Proc Natl Acad Sci U S A* 1962, **48**:1238-1245.

18. Militello KT, Patel V, Chessler AD, Fisher JK, Kasper JM, Gunasekera A, Wirth DF: **RNA polymerase II synthesizes antisense RNA in Plasmodium falciparum**. *Rna* 2005, **11**(4):365-370.
19. Bozdech Z, Zhu J, Joachimiak MP, Cohen FE, Pulliam B, DeRisi JL: **Expression profiling of the schizont and trophozoite stages of Plasmodium falciparum with a long-oligonucleotide microarray**. *Genome Biol* 2003, **4**(2):R9.
20. Yang E, van Nimwegen E, Zavolan M, Rajewsky N, Schroeder M, Magnasco M, Darnell JE, Jr.: **Decay rates of human mRNAs: correlation with functional characteristics and sequence attributes**. *Genome Res* 2003, **13**(8):1863-1872.
21. Ruvolo V, Altszuler R, Levitt A: **The transcript encoding the circumsporozoite antigen of Plasmodium berghei utilizes heterogeneous polyadenylation sites**. *Mol Biochem Parasitol* 1993, **57**(1):137-150.
22. Oguariri RM, Dunn JM, Golightly LM: **3' gene regulatory elements required for expression of the Plasmodiumfalciparum developmental protein, Pfs25**. *Mol Biochem Parasitol* 2006, **146**(2):163-172.
23. Beissbarth T, Speed TP: **GOstat: find statistically overrepresented Gene Ontologies within a group of genes**. *Bioinformatics* 2004, **20**(9):1464-1465.
24. Kim CC, Falkow S: **Significance analysis of lexical bias in microarray data**. *BMC Bioinformatics* 2003, **4**:12.
25. Martin RE, Henry RI, Abbey JL, Clements JD, Kirk K: **The 'permeome' of the malaria parasite: an overview of the membrane transport proteins of Plasmodium falciparum**. *Genome Biol* 2005, **6**(3):R26.
26. de Rojas MO, Wasserman M: **Temporal relationships on macromolecular synthesis during the asexual cell cycle of Plasmodium falciparum**. *Trans R Soc Trop Med Hyg* 1985, **79**(6):792-796.
27. Gritzmacher CA, Reese RT: **Protein and nucleic acid synthesis during synchronized growth of Plasmodium falciparum**. *J Bacteriol* 1984, **160**(3):1165-1167.
28. Cleary MD, Meiering CD, Jan E, Guymon R, Boothroyd JC: **Biosynthetic labeling of RNA with uracil phosphoribosyltransferase allows cell-specific microarray analysis of mRNA synthesis and decay**. *Nat Biotechnol* 2005, **23**(2):232-237.
29. Lotan R, Bar-On VG, Harel-Sharvit L, Duek L, Melamed D, Choder M: **The RNA polymerase II subunit Rpb4p mediates decay of a specific class of mRNAs**. *Genes Dev* 2005, **19**(24):3004-3016.
30. Duttagupta R, Tian B, Wilusz CJ, Khounh DT, Soteropoulos P, Ouyang M, Dougherty JP, Peltz SW: **Global analysis of Pub1p targets reveals a coordinate control of gene expression through modulation of binding and stability**. *Mol Cell Biol* 2005, **25**(13):5499-5513.
31. Mor'e J (ed.): **The Levenberg-Marquardt Algorithm: Implementation and Theory**. Berlin/Heidelberg/New York: Springer-Verlag; 1978.
32. Eisen MB, Spellman PT, Brown PO, Botstein D: **Cluster analysis and display of genome-wide expression patterns**. *Proc Natl Acad Sci U S A* 1998, **95**(25):14863-14868.
33. Sambrook J, Fritsch EF, Maniatis T: **Molecular cloning, a laboratory manual**, vol. 2, second edn. Cold Spring Harbor: Cold Spring Harbor press; 1989.

Figure 1. Nuclear run-on analysis shows that actinomycin D halts transcription in *P. falciparum.* Actinomycin D was added to synchronous cultures in the ring and late schizont stages. Time points were then taken before addition of actinomycin D and then at 0, 7.5 and 15 minute intervals after addition of drug. The samples were normalized such that the no actinomycin D sample was normalized to 100% transcription.

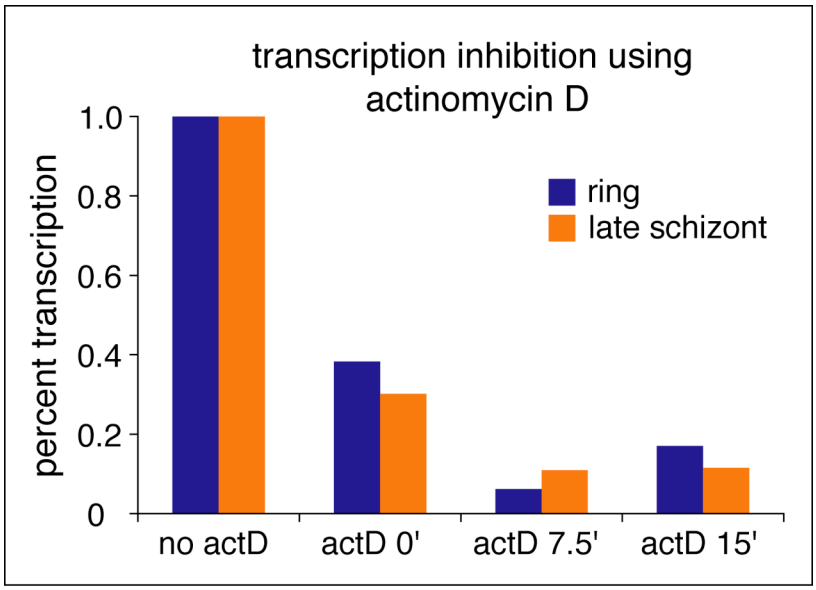

Figure 2. Schematic of the microarray experiment to determine half-lives through the life cycle. Four separate time course experiments were conducted at 12 hour intervals using a single source culture of synchronized parasites. Numbers in red represent the hour post invasion when actinomycin D was added in relationship to the previously published transcriptome experiment. Total RNA was subsequently harvested at the indicated time points. These samples were reverse transcribed into cDNA and hybridized to DNA microarrays. Specific spiked controls were included to determine correct normalization during microarray scanning.

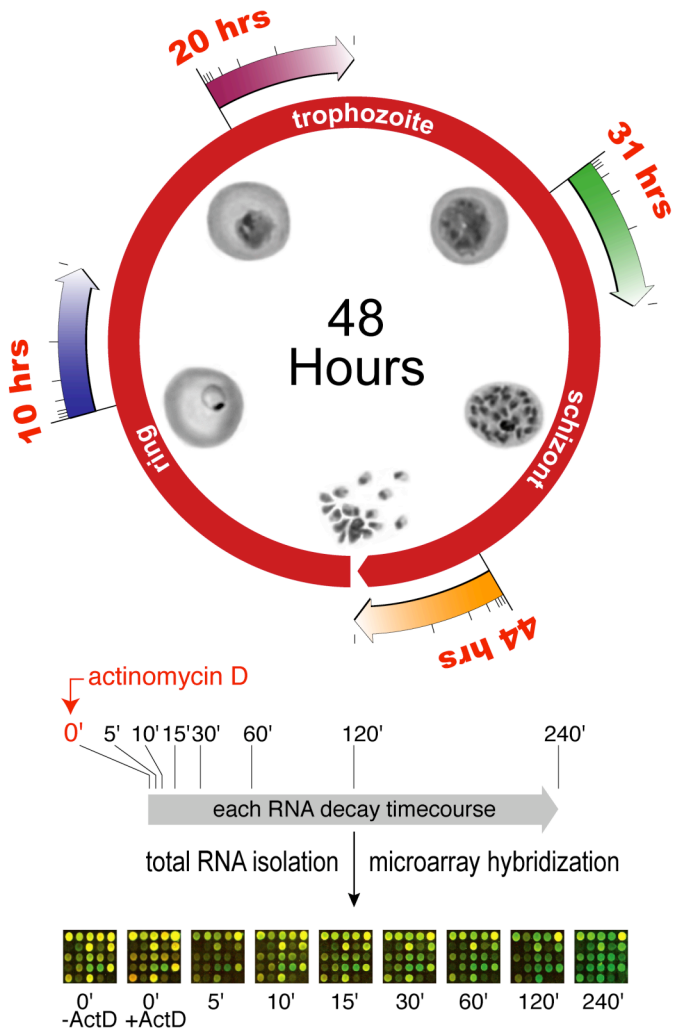

Figure 3. Examples of mRNA decay profiles for each stage determined by microarray analysis. Four example genes were chosen to demonstrate the range of half-lives that can be measured in this experiment. The black dots represent data points from each of the microarray replicates for that time point including the 0 time point with and without actinomycin D treatment. The colored lines represent the fitted decay curve. The half life for each example is listed.

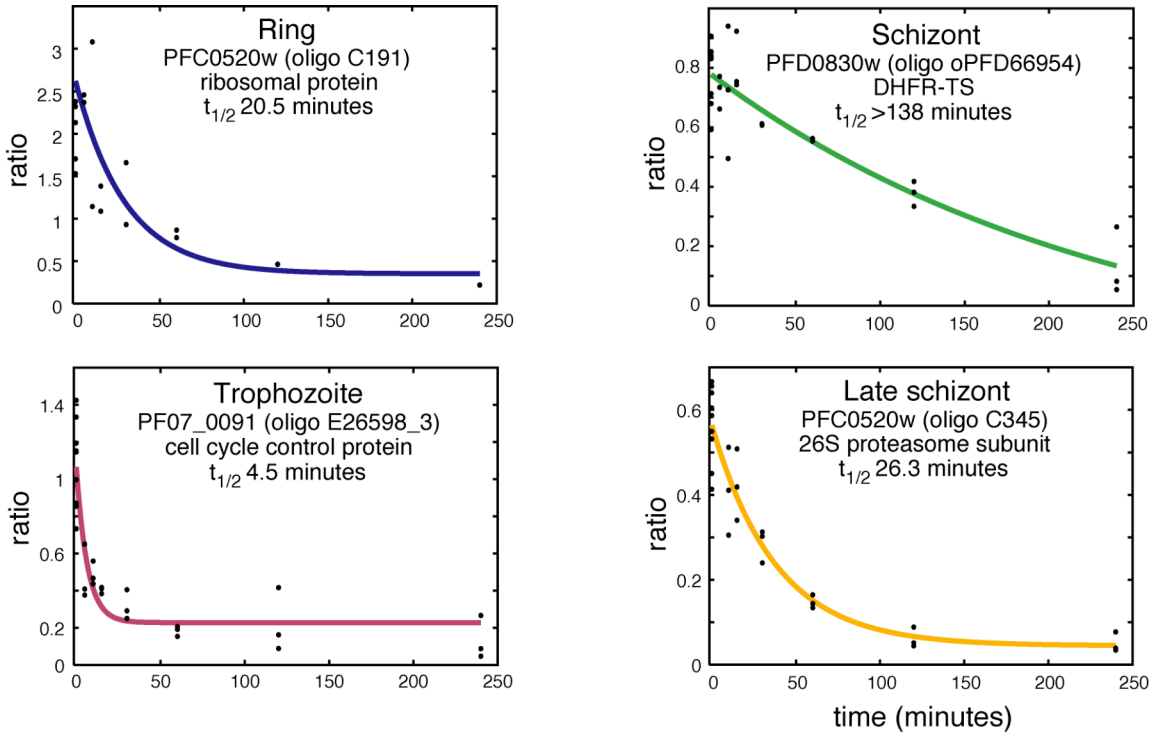

Figure 4. The distribution of mRNA half-lives changes for each stage of erythrocytic development. Both the histogram and the graph of mean half-lives for each stage (inset) reveal that half-lives increase on a global scale over the course of the IDC.

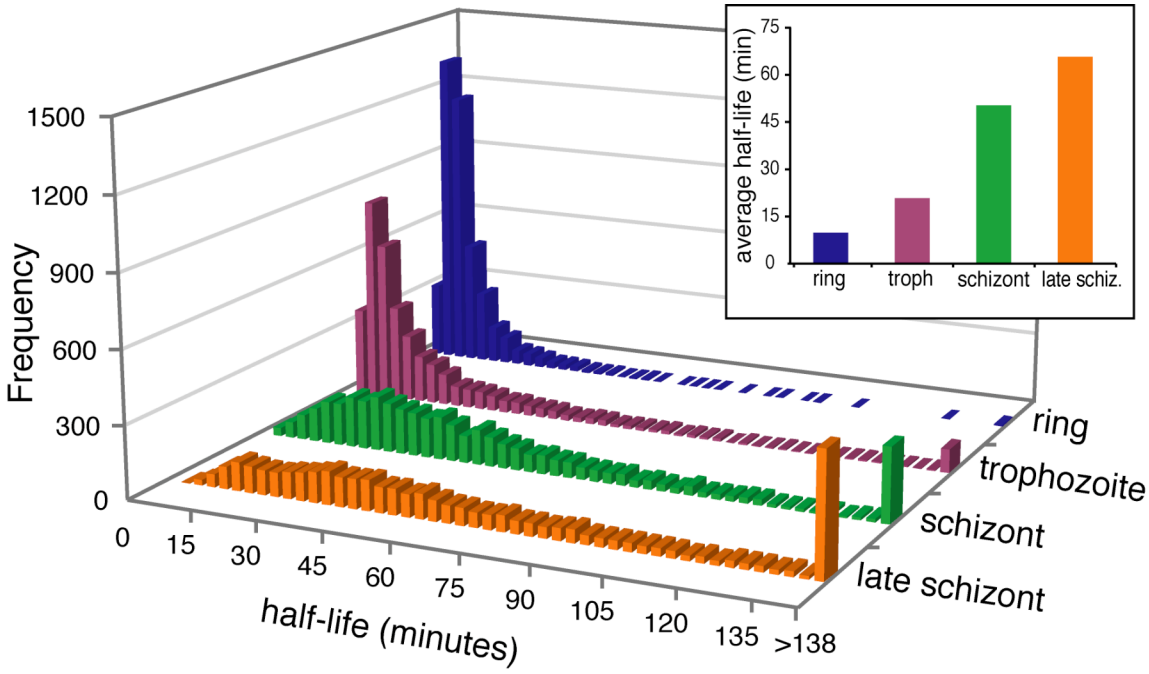

Figure 5. Comparison of decay rate calculated by microarray and by Northern blot. The half-lives for PFB0760w and PF13_0116 were verified by Northern blot analysis (quantified by PhosphorImager) for the ring and late schizont stages using total RNA from the same experiment. All of the microarray replicates were used to calculate the decay rate from the microarrays.

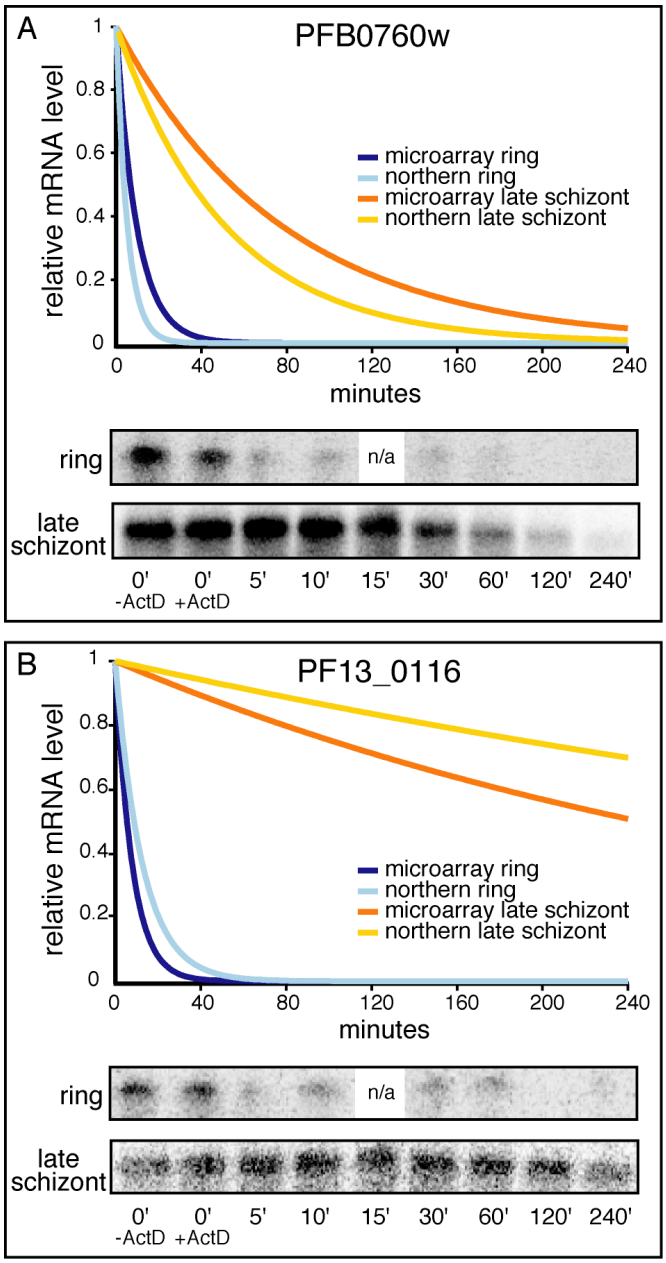

Figure 6. *K*-means clusters of the half-life data for each stage. Genes were clustered into 10 *k*-means clusters using the $\log_2$ transformed half-life (minutes) in each stage. The average half-life was used for genes represented by more than one oligo (Materials and Methods). In the plot to the right of each *k*-means cluster, the average decay profile for each group is displayed (red line) with the average decay profile for the entire data set (gray line filled down). The *x*-axis represents the four stages progressing through the life cycle from rings to late schizonts. The *y*-axis represents half-life from 0-100 minutes. $\Delta t_{1/2}$ represents the average half-life difference between the late schizont stage and the ring stage for that group (late schizont half-life – ring half-life). On the right is the top two most significant GO terms for each *k*-means cluster (GoStat was used for this analysis).

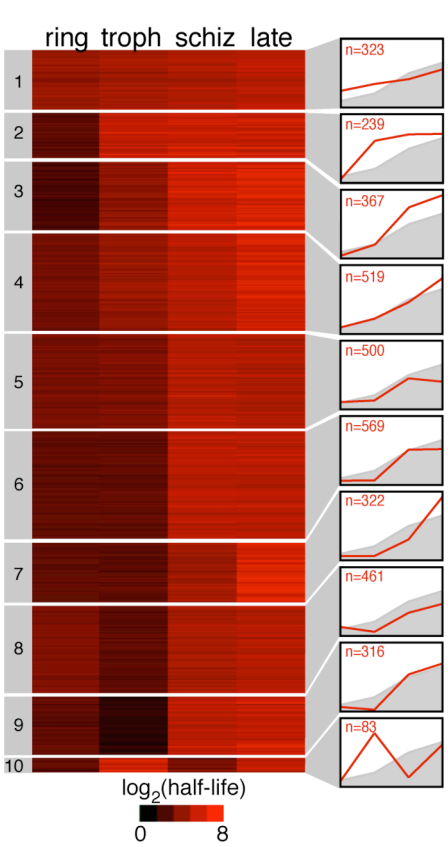

$\Delta t_{1/2}$	GO term	p value
31'	ribosome	1.28×10^{-16}
	protein biosynthesis	1.20×10^{-8}
66'	small ribosomal subunit	6.54×10^{-4}
	mutualism through parasitism	8.67×10^{-4}
88'	response to chemical stimulus	3.56×10^{-3}
	interaction with host	9.32×10^{-3}
72'	generation of precursor metabolites and energy	4.65×10^{-4}
	cellular catabolism	2.66×10^{-3}
30'	nucleolus	3.67×10^{-5}
	rRNA metabolism	1.89×10^{-4}
46'	RNA elongation	4.10×10^{-3}
	endopeptidase Clp activity	4.10×10^{-3}
86'	protein kinase activity	4.56×10^{-3}
	chromatin remodeling	4.58×10^{-3}
34'	potassium ion transport	2.18×10^{-3}
63'	none	
54'	host	3.28×10^{-5}
	antigenic variation	1.47×10^{-4}

Table 1. Putative decay components in *P. falciparum* were identified using known factors from human and yeast. Orthologs were identified using a simple reciprocal best BLASTP match between *P. falciparum* and *S. cerevisiae* and between *P. falciparum* and human sequences. Orthologs could not be found for those genes with question marks. Components with asterisks were identified only when the human sequence was used for the query sequence. Those *P. falciparum* proteins in bold are described in PlasmoDB either as hypothetical proteins, or in the case of PF10_0314 assigned a function other than the one relevant here.

Gene	PlasmoDB ID	Description
Deadenylation components		
Ccr4	**PFE0980c**	catalytic subunit of the Ccr4/Pop2 deadenylase complex
Pop2	**MAL8P1.104**	component of the Ccr4/Pop2 deadenylase complex
Not1	**PF11_0049**	component of the Ccr4/Not complex
Not2	**PF11_0297**	component of the Ccr4/Not complex
Not3	?	component of the Ccr4/Not complex
Not4	**PFL1705w**	component of the Ccr4/Not complex
Not5	**PF10_0062**	component of the Ccr4/Not complex
Caf130	?	component of the Ccr4/Not complex
Caf40	PFE0375w	component of the Ccr4/Not complex
PARN	**PF14_0413***	major deadenylase in mammals
Pab1	PFL1170w	polyA binding protein
Pan2	?	component of the Pan2/Pan3 deadenylase complex
Pan2	?	component of the Pan2/Pan3 deadenylase complex
Decapping components		
Dcp1	**PF10_0314***	component of the Dcp1/Dcp2 decapping complex
Dcp2	**Pf13_0048**	catalytic subunit of the Dcp1/Dcp2 decapping complex
DcpS/Dcs1	?	scavenger decapping enzyme
Dhh1	PFC0915w	helicase-roles in deadenylation and decapping
Lsm1	**PF11_0255**	involved in decapping
Lsm2	PFE1020w	involved in decapping
Lsm3	PF08_0049	involved in decapping
Lsm4	PF11_0524	involved in decapping
Lsm5	PF14_0411	involved in decapping
Lsm6	PF13_0142	involved in decapping
Lsm7	PFL0460w	involved in decapping
Exosome components		
Csl4	MAL7P1.104	exosome subunit
Dis3/Rrp44	**MAL13P1.28**	exosome subunit-RNase II domain
Mtr3	?	exosome subunit-RNase PH domain

Rrp4	PFD0515w	exosome subunit-hydrolytic exonuclease
Rrp40	**MAL13P1.36**	exosome subunit-hydrolytic exonuclease
Rrp42	**MAL13P1.20**	exosome subunit-RNase PH domain
Rrp43	?	exosome subunit-RNase PH domain
Rrp45	PF13_0340	exosome subunit-RNase PH domain
Rrp46	?	exosome subunit-RNase PH domain
Rrp6	PF14_0473	exosome subunit found only in the nucleus
Ski2	PFI0480w	helicase associated with the exosome and Ski complex
Ski3/Ski5	?	associated with exosome and Ski complex
Ski6/Rrp41	PF14_0256	exosome subunit-RNase PH domain
Ski7	?	associated with exosome and Ski complex
Ski8	?	associated with exosome and Ski complex
5' to 3' decay		
Xrn1	PFI0455w/ **PF11_0074**	5' to 3' exonuclease-cytoplasmic
Rat1	PFI0455w/ **PF11_0074**	5' to 3' exonuclease-nuclear

Table 2. Average half-lives and standard deviations for each stage.

	half-life in minutes	standard deviation in minutes	standard deviation for oligos within a single ORF
ring	9.5	9.9	4.6
trohpozoite	20.5	28.5	9.9
schizont	49.9	37.3	21.9
late schizont	65.4	42.6	22.2

Additional data files

Dataset 1 (excel). The complete dataset containing initial ratio (A_0), final ratio (B) and half-life ($t_{1/2}$) as well as the asymptotic standard errors for each of these parameters.

Dataset 2 (excel). The complete dataset containing a list of oligos that did not pass the quality control filters in each stage. The specific filter or filters these oligos did not pass are listed.

Dataset 3 (excel). A complete list of all the significant GO terms and associated p-values found in each of the k-means clusters.

Chapter 3: Tetracyclines Specifically Target the Apicoplast of the Malaria Parasite *Plasmodium falciparum*

This chapter is a reprint from the following reference:

Dahl, E.L., Shock, J.L., Shenai, B.R., Gut, J., DeRisi, J.L. and Rosenthal, P.J. (2006) Tetracyclines specifically target the apicoplast of the malaria parasite *Plasmodium falciparum*. Antimicrobial Agents and Chemotherapy 50(9): 3124–3131.

Author contributions:

Erica Dahl obtained the data for figures 1, 2, 4, 5, 6, and 7. Jennifer Shock performed the microarray experiments described in figure 3. Philip Rosenthal and Joseph DeRisi supervised the research.

Joseph L. DeRisi, thesis advisor

Abstract

Tetracyclines are effective but slow-acting antimalarial drugs whose mechanism of action remains uncertain. To characterize the antimalarial mechanism of tetracyclines, we evaluated their stage-specific activities, impacts on parasite transcription, and effects on two predicted organelle targets, the apicoplast and the mitochondrion, in cultured *Plasmodium falciparum*. Antimalarial effects were much greater after two 48-h life cycles than after one cycle, even if the drugs were removed at the end of the first cycle. Doxycycline-treated parasites appeared morphologically normal until late in the second cycle of treatment but failed to develop into merozoites. Doxycycline specifically impaired the expression of apicoplast genes. Apicoplast morphology initially appeared normal in the presence of doxycycline. However, apicoplasts were abnormal in the progeny of doxycycline-treated parasites, as evidenced by a block in apicoplast genome replication, a lack of processing of an apicoplast-targeted protein, and failure to elongate and segregate during schizogeny. Replication of the nuclear and mitochondrial genomes and mitochondrial morphology appeared normal. Our results demonstrate that tetracyclines specifically block expression of the apicoplast genome, resulting in the distribution of nonfunctional apicoplasts into daughter merozoites. The loss of apicoplast function in the progeny of treated parasites leads to a slow but potent antimalarial effect.

Introduction

Plasmodium falciparum causes an estimated half billion cases of malaria, resulting in over a million deaths, each year [1, 2]. Tetracyclines are effective, albeit slow-acting, antimalarials that are used in combination with a more rapidly acting drug to treat malaria [3] and for antimalarial chemoprophylaxis [4]. The antimalarial mechanism of action of tetracyclines remains undefined. Consistent with their slow clinical activity, tetracyclines exert in vitro antimalarial effects slowly, requiring incubation with cultured *P. falciparum* beyond a single 48-h asexual cycle for maximal effects [5]. Tetracyclines exert antibacterial activity by inhibiting prokaryotic translation [6]. However, in the eukaryote *P. falciparum*, protein synthesis is broadly inhibited by tetracyclines only at much higher concentrations than those required to block parasite growth [7], suggesting that their antimalarial effects are due to action against a target other than cytosolic ribosomes.

Early studies of the mechanism of action of tetracyclines against *P. falciparum* focused on the parasite's single mitochondrion as the likely target [8, 9]. However, these studies preceded the identification of the apicoplast, an organelle of uncertain function that is related to the chloroplast of plant cells [10, 11]. The mitochondrion and the apicoplast each contain their own genome, encoding prokaryote-like ribosomal RNAs, tRNAs, and some proteins [12, 13]. In addition, several hundred nuclear genes encode proteins targeted to the apicoplast or the mitochondrion [14-18]. The apicoplast houses enzymes involved in type II fatty acid synthesis, a nonmevalonate pathway for isoprenoid biosynthesis, and heme-biosynthetic pathways [19]. The mitochondrion maintains a mitochondrial membrane potential and houses a complete citric acid cycle. However, its

role in energy generation is still unclear, since a link from the citric acid cycle to the electron transport chain remains to be defined [20]. The mitochondrion does house a number of enzymes involved in pyrimidine and heme biosynthesis, and disruption of either organelle would be expected to block critical biosynthetic pathways. Since both organelles contain prokaryote-like ribosomal components, either is a potential target of tetracyclines.

To better characterize the antimalarial mechanism(s) of tetracyclines, we evaluated their activities over two 48-h parasite life cycles. We then evaluated the effects of doxycycline on parasite gene expression by microarray analysis and on specific mitochondrion and apicoplast self-maintenance functions. Our results are consistent with a model in which doxycycline specifically inhibits the production of proteins encoded by the apicoplast genome, leading to a subsequent loss of apicoplast function and a delayed but potent antimalarial effect.

Material and Methods

Malaria parasite and culture

P. falciparum parasites were cultured in human erythrocytes maintained at 2% hematocrit in RPMI 1640 medium with 0.5% (wt/vol) AlbuMAX II (Invitrogen-Gibco) in 92% N_2, 5% CO_2, and 3% O_2 [21]. Synchrony was maintained by serial sorbitol treatments [22]. Strain W2 was used for the determination of 50% inhibitory concentrations (IC_{50}s) and microscopy, and 3D7 was used in microarray and Southern analyses. Parasites stably expressing green fluorescent protein fused to an acyl carrier protein apicoplast-targeting sequence (ACP_I-GFP), kindly provided by Geoff McFadden

[23], were maintained in medium containing 100 nM pyrimethamine. Dually transfected parasites stably expressing a red fluorescent protein fused to an acyl carrier protein apicoplast-targeting signal and a yellow fluorescent protein fused to a citrate synthetase mitochondrial targeting signal (ACP_I-DsRed and CS_I-YFP), also kindly provided by Geoff McFadden [24], were maintained in medium containing 5 nM WR99210.

Unless stated otherwise, all doxycycline studies were carried out as follows. Synchronized parasites were treated at the late ring/early trophozoite stage (approximately 20 h postinvasion) with 1 μM doxycycline or an equivalent volume of dimethyl sulfoxide (DMSO) for 24 h, until they reached the late schizont stage. The parasites were then subcultured into fresh medium and allowed to invade new erythrocytes and progress through a second cycle in the absence of drug. The medium was replaced every 24 h. Doxycycline, minocycline, tetracycline, and pyrimethamine were from Sigma. WR99210 was the gift of David Jacobus (Jacobus Pharmaceuticals).

Antiparasitic effects of tetracyclines

W2 strain parasites were cultured in 96-well plates at initial parasitemias of 1% for 48-h and 0.2% for 96-h drug studies. Serial dilutions of tetracyclines (100 μM to 1 nM; dissolved in DMSO) and chloroquine (dissolved in water) were prepared in complete medium. Equivalent volumes of DMSO were included as controls.

The IC_{50} of each drug was determined by comparing parasite counts by flow cytometry and the uptake of [^{3}H]hypoxanthine by standard methods. For flow cytometry, after incubation with the drugs, infected erythrocytes were fixed in 1% paraformaldehyde in phosphate-buffered saline (PBS) for 48 h, permeabilized with 0.1% Triton X-100, and

stained with 1 nM YOYO-1 (Molecular Probes). Parasitemias were determined from dot plots (forward scatter versus fluorescence) acquired on a FACSort cytometer using CELLQUEST software (Becton Dickinson). Hypoxanthine uptake assays were performed essentially as described previously [25]. Briefly, late-ring-stage-infected erythrocytes were cultured in medium containing 10 μCi/ml [^{3}H]hypoxanthine (NEN Life Sciences) for 48 h and then harvested and washed using a PHD Cell Harvester (Cambridge Technology Inc.). ^{3}H incorporation was assessed in a Beckman LS 6000IC scintillation counter (Beckman Coulter Inc.). IC_{50}s were calculated from variable-slope sigmoidal dose-response curves using GraphPad Prism version 3.00 for Windows (GraphPad Software).

Microscopy

For light microscopy, thin smears were prepared, stained with Giemsa stain, and photographed using a SPOT Flex Color Mosaic Digital Camera (Diagnostic Instruments) on a Nikon Optiphot microscope. For electron microscopy, infected erythrocytes were washed in PBS, fixed in Karnovsky's solution (1% paraformaldehyde, 3% glutaraldehyde, 0.1 M sodium cacodylate buffer, pH 7.4) for 4 h at room temperature, and then stored at 4°C until they were analyzed. Fixed samples were postfixed in reduced OsO_4 (2% OsO_4 plus 1.5% potassium ferrocyanide; Sigma) and stained en bloc with uranyl acetate before being dehydrated in ethanol, cleared in propylene oxide, and embedded in Eponate 12 (Ted Pella Co). Thin sections were cut with a Leica ultracut UCT microtome, stained with uranyl acetate and Reynold's lead, and examined with a Philips Tecnai 10 electron microscope. Photographs were scanned using a CanoScan

N6700 (Canon).

For fluorescence microscopy of ACP_l-GFP parasites, infected erythrocytes were fixed in 1% formaldehyde, 0.1% gluteraldehyde, and a 1:400 dilution of DAPI (4′,6′-diamidino-2-phenylindole) nuclear stain (Molecular Probes) in PBS; pipetted onto poly-l-lysine-coated microscope slides; incubated for 30 min at room temperature; washed in PBS; air dried; and overlaid with mounting solution (10% Mowiol 4-88, 25% glycerol, 2.5% 1,4-diazobicyclo-[2.2.2]-octane, 0.1 M Tris-HCl, pH 8.5) [26] and a coverslip. For fluorescence microscopy of live ACP_l-DsRed CS_l-YFP parasites, infected erythrocytes were rinsed in serum-free RPMI medium and allowed to attach to a poly-l-lysine-coated microscope slide for 30 min. The slides were then rinsed in serum-free RPMI medium, overlaid with a coverslip, and imaged immediately. Fluorescent images were captured using a SPOT Flex Color Mosaic Digital Camera (Diagnostic Instruments) on a Nikon Optiphot microscope. Merged images were assembled and optimized (background corrections and gamma adjustments) using SPOTsoftware version 4.5 (Diagnostic Instruments). For all microscopy, final figures were prepared in Adobe Photoshop version 5.5.

Microarray analysis

Parasites were incubated with doxycycline for 20 h and then subcultured and maintained in drug-free medium for an additional 35 h. Infected erythrocytes were collected every 5 h, lysed with 0.1% saponin for 5 min, centrifuged at 12,000 × *g* at 4°C, flash frozen in an ethanol-dry ice bath, and stored at −80°C. Total parasite RNA was harvested using TRIzol reagent (Invitrogen). For each sample, 12 μg of total parasite

RNA was reverse transcribed into cDNA containing amino-allyl-dUTP (Ambion) using SuperScript II RNase H-Reverse Transcriptase (Invitrogen) and then coupled to succidimyl ester Cy5 dye (Amersham) as described previously [27]. Cy5-labeled sample cDNA and a reference pool of Cy3-labeled cDNA representing all life cycle stages were competitively hybridized to a *P. falciparum* 70-mer microarray as described previously [28]. The microarrays were scanned using a GenePix 4000B scanner, and images were analyzed using GenePix3 Software (Molecular Devices, Inc.), stored, and normalized using the NOMAD database (https://ucsf-nomad.sourceforge.net). Expression data were log transformed and mean centered. Self-organizing map and cluster analysis was performed using Cluster software and visualized using Treeview [29].

Southern hybridization

Total DNA was isolated from schizont stage parasites using the Puregene DNA Purification kit (Gentra) and digested with XmnI and SacI, and samples (5 μg per lane) were electrophoresed on a 0.7% agarose gel and transferred to a Hybond N+ nylon membrane (Amersham Biosciences).

For probes, we amplified a 511-bp fragment of the mitochondrial genome between nucleotides 4998 and 5509 (which includes the putative ribosomal-DNA sequences *ssuD* and *lsuA* [12]) (primers, 5′ ACGCTGACTTCCTG 3′ and 5′ AGAAAACAGTCGGTG 3′) from genomic *P. falciparum* DNA, a 573-bp fragment of the apicoplast gene *tufA* (primers 5′ ATAGGAGCCACACA 3′ and 5′ TCCGGATTGTGCTT 3′) from genomic *P. falciparum* DNA, and a 500-bp fragment of the nuclear gene *falcipain-3* from the plasmid pTOPO-FP3 [30] (primers 5′

TACCATGGTACATAAGCTTCTGTTCCAATTGAACAA 3′ and 5′ TTAGAATTCTCATGTTGGGCTTTTAGTAGT 3′). Probes were gel purified and extracted using the QIAGEN Gel Extraction Kit and then labeled with [α-^{32}P]dATP using the Megaprime DNA Labeling System (Amersham Biosciences). Blots were prehybridized for 5 h in RapidHyb hybridization buffer (Amersham Biosciences) at 56°C and hybridized overnight at 65°C with the probes. The blots were then washed twice at 25°C in 2× SSC (SSC is 0.15 M NaCl/0.15 M Na citrate, pH 7.0), 0.1% sodium dodecyl sulfate (SDS); once at 55°C in 1× SSC, 0.1% SDS; and once at 60°C in 1× SSC, 0.1% SDS before visualization by autoradiography.

Immunoblots

ACP_I-GFP-containing parasites were isolated from erythrocytes with saponin, and denatured samples (5×10^7 parasites per lane) were electrophoresed on 12.5% polyacrylamide gels under reducing conditions. Proteins were transferred to polyvinylidene difluoride membranes and probed with mouse anti-GFP antibodies (Molecular Probes; 1:400), followed by alkaline phosphatase-conjugated donkey anti-mouse secondary antibody (Jackson ImmunoResearch Laboratories; 1:10,000) using standard procedures. Immunoblots were developed using the Western-*Star* Chemiluminescent Immunoblot Detection System with CDP-*Star* substrate (Applied Biosystems). The blots were stripped and reprobed with a 1:10,000 dilution of rat anti-falcipain-3 antibody [30], followed by alkaline phosphatase-conjugated goat anti-rat antibody (Jackson ImmunoResearch Laboratories; 1:10,000).

Nucleotide sequence accession numbers

All microarray data are available at the Gene Expression Omnibus database (http://www.ncbi.nlm.nih.gov/geo/), accession no. GSE5267.

Results

Delayed antimalarial activities of tetracyclines

We evaluated the antimalarial activities of tetracycline, doxycycline, and minocycline over two 48-h parasite life cycles with standard assays, comparing either the uptake of hypoxanthine or the multiplication of parasites between treated and control parasites. The concentrations of these antibiotics in human plasma after standard dosing ranges between 4.7 and 5.6 μM for tetracycline, 3.7 and 4.3 μM for doxycycline, and 5.0 and 7.7 μM for minocycline [31]. When assessed based on activity during a single cycle, the tetracyclines were relatively inactive, with IC_{50}s above clinically relevant concentrations (Table 1). The tetracyclines showed much greater potency when assessed after a second cycle, consistent with earlier reports of slow action against malaria parasites [5, 32], with IC_{50}s at concentrations that are achievable with standard dosing of these agents. Remarkably, the increased potency after a second cycle was seen even if the tetracyclines were removed from culture after the first cycle of incubation (Table 1). Since doxycycline is the most widely used tetracycline to treat and prevent malaria, we chose it as our model compound for further characterizing the antimalarial actions of tetracyclines. To characterize stage-specific activity, we cultured parasites in doxycycline over different portions of the first cycle and evaluated the subsequent effects (Fig. 1).

Trophozoite and early schizont stage parasites were most sensitive to doxycycline; incubations during the ring or late schizont stage had much less effect.

Doxycycline-treated parasites appeared to be morphologically normal through the entire first 48-h erythrocytic cycle (Fig. 2A), producing merozoites that invaded erythrocytes and formed normal-appearing daughter ring stage parasites. The parasites continued to develop through the second cycle and initiated schizogeny, with the appearance of multiple daughter nuclei. However, the mature schizonts became increasingly abnormal and failed to progress to merozoite release and subsequent erythrocyte invasion. Electron micrographs also showed that mature schizonts during the initial cycle of incubation with doxycycline (40 h) appeared to be normal. In the second cycle (88 h), doxycycline-treated schizonts lacked defined intracellular compartments, and many displayed abnormal vacuolation (Fig. 2B). The observed blocks in merozoite maturation and egress at 96 h were apparent even if drugs were removed after 48 h of incubation (not shown).

Expression of genes encoded by the apicoplast is specifically disrupted by doxycycline

To identify specific targets of doxycycline, we compared the transcriptomes of doxycycline-treated and control parasites over a 55-h period, beginning in early trophozoites (treatment began approximately 18 h postinvasion) through the mature trophozoite stage of the following cycle (approximately 24 h postinvasion). The patterns of gene expression in the doxycycline-treated and control parasites were remarkably similar (Fig. 3A). Using an overview gene set derived from a previously described

intraerythrocytic developmental cycle transcriptome [28], we calculated the average correlation of expression profiles between treated and untreated cultures to be 0.80, indicating very little variation in gene expression following doxycycline treatment.

Subtle differences between microarray time courses can be detected by calculating the relative expression ratio between two samples at each time point [33, 34]. We calculated the relative ratios between the untreated and treated time courses and then filtered the data set for array features (70-mers representing *P. falciparum* coding regions) representing genes that were consistently underexpressed in doxycycline-treated parasites, using modest criteria (greater than 1.6-fold underexpression at at least half of the time points). Only 104 array features (less than 2%) met these criteria. To assess whether any functional groups of genes were overrepresented in this set relative to the entire data set, we used the LACK software tool to calculate the statistical significance of lexical bias in the PlasmoDB annotations of our underexpressed gene set [35]. The annotation "plastid" (signifying genes on the plastid genome), but no other annotation term, was significantly overrepresented ($P < 10^{-6}$, as calculated by binomial distribution) in our set of underexpressed genes. Indeed, essentially all of the plastid genes represented on our microarray were consistently underexpressed (Fig. 3B).

To assess the degree of underexpression relative to the distribution of all genes, we calculated a histogram of the average underexpression ratio for all unique array features at the hours of peak plastid expression (20 h and 55 h) and plotted the positions of the plastid genes (Fig. 3C). Apicoplast genes were clearly underexpressed relative to other features. Genes carried by the mitochondrion and nuclear genes whose products are targeted to the apicoplast or mitochondrion were unaffected by doxycycline treatment

(not shown). Thus, doxycycline treatment specifically disrupts the expression of apicoplast genes.

Replication of apicoplast DNA is disrupted in the progeny of doxycycline-treated parasites

The apicoplast and mitochondrial genomes of *P. falciparum* replicate at the beginning of schizogeny, at the same time as the nuclear genome [36-38]. We compared the replication of nuclear, apicoplast, and mitochondrial genomes in doxycycline-treated and control schizonts. Parasites were incubated with doxycycline during a single cycle, and schizont DNA was extracted and evaluated during this and the subsequent cycle by Southern analysis utilizing probes for the nuclear, apicoplast, and mitochondrial genomes. In the presence of doxycycline, replication of the three genomes was the same as in control schizonts (Fig. 4). In the following cycle, replication of apicoplast DNA, but not nuclear or mitochondrial DNA, was markedly reduced during schizogeny. These results demonstrate that the progeny of doxycycline-treated parasites are unable to replicate the apicoplast genome.

Apicoplast segregation is disrupted in the progeny of doxycycline-treated parasites

We treated *P. falciparum* expressing ACP_I-GFP [23] with doxycycline for a single cycle and then evaluated the morphology of the apicoplasts in trophozoite and schizont stages in this and the subsequent cycle (Fig. 5). In control parasites, the apicoplast elongated into a branched morphology in schizonts before segregating into merozoites, as reported previously [23, 24]. In doxycycline-treated parasites, elongation,

branching, and segregation of apicoplasts did not appear to be altered. Quantitation by flow cytometry confirmed that the numbers of progeny containing GFP-labeled apicoplasts were the same in doxycycline-treated and control parasites (not shown). The apicoplast was visualized through most of the life cycle in these daughter parasites, indicating that the organelle was intact and that apicoplast-targeting signals were functional. However, as the parasites progressed to schizonts, the elongation, branching, and segregation of apicoplasts were disrupted, and the parasites failed to develop beyond the schizont stage.

To further evaluate the effects of doxycycline on apicoplast and mitochondrial morphologies, we treated parasites stably expressing both ACP_I-DsRed and CS_I-YFP [24] with doxycycline as described above. Both the apicoplast and the mitochondrion displayed typical [24, 39, 40] elongation, branching, and segregation patterns in the presence of doxycycline. In the progeny of doxycycline-treated parasites, the apicoplast was visible, indicating that the organelle was present and that targeting of DsRed was normal, as had been observed for GFP. However, apicoplast elongation, branching, and segregation were again disrupted as the parasites initiated schizogeny (Fig. 6). In contrast, the mitochondrion appeared to develop normally, forming elongated and elaborately branched structures in the progeny of doxycycline-treated parasites.

Processing of apicoplast-targeted proteins is disrupted in the progeny of doxycycline-treated parasites

Apicoplast-targeted *P. falciparum* proteins contain a leader sequence that is cleaved upon delivery to the apicoplast [41]. We analyzed the processing of apicoplast-

targeted GFP by immunoblot analysis with an anti-GFP antibody. Expression and processing of ACP_I-GFP were the same in doxycycline-treated and control parasites during the first cycle. However, processing was blocked in the progeny of doxycycline-treated parasites, but not controls (Fig. 7). The expression and processing of the nuclear-encoded cysteine protease falcipain-3 was unaffected by doxycycline, demonstrating that the inability of parasites to process ACP_I-GFP was due to a specific abnormality in apicoplast function rather than a general defect in protein processing.

Discussion

Tetracyclines are effective antimalarials, but their mechanism of action is unclear. Since these agents block prokaryotic protein synthesis, it has been proposed that they disrupt the mitochondrion or the apicoplast, both of which include prokaryotic ribosomal subunits in their genomes. We have shown that both the mitochondrion and apicoplast appear normal through a cycle of treatment with doxycycline, that these organelles are successfully segregated into daughter parasites, and that they remain intact in the progeny of treated parasites. However, doxycycline specifically blocks the expression of apicoplast genes, leading to the distribution of nonfunctional apicoplasts into daughter parasites and a subsequent block in parasite development. These results indicate that the site of action of tetracyclines is the apicoplast but that loss of apicoplast function is not apparent until late in the cycle following treatment, explaining the slow action of these drugs.

Previous work on the antimalarial effects of tetracyclines demonstrated increased efficacy with prolonged treatment [5, 32, 42]. Doxycycline inhibited global protein

synthesis only at suprapharmacological concentrations [7], arguing against cytosolic ribosomes as a target for tetracyclines in vivo. Early work examining the mitochondrion as a potential target of tetracyclines demonstrated decreased mitochondrial uptake of rhodamine 123 after 72 h [8]. However, this observation may have reflected secondary toxicity to the mitochondrion following primary effects of the drug. Other studies demonstrating depression of mitochondrial enzyme activity [9] and a block in both apicoplast and mitochondrial transcription [43] assessed tetracyclines at concentrations well above those that are clinically achievable.

The slow action of tetracyclines against *P. falciparum* was observed even if trophozoite and early schizont stage parasites were treated for as little as 12 h. Apicoplasts in treated parasites initially appeared morphologically normal, replicated their genomes, processed imported proteins, and segregated into developing merozoites. Doxycycline specifically disrupted the expression of apicoplast genes. However, most of the proteins predicted to be required for apicoplast function are encoded by the nuclear genome [17], so the apicoplast would be expected to perform most functions normally as long as its import machinery remained intact. We propose that, though doxycycline does not prevent apicoplast function initially, the apicoplasts inherited by the progeny of doxycycline-treated parasites contain insufficient levels of apicoplast-encoded proteins required for the importation and processing of the several hundred nuclear genes needed for normal function. This loss of apicoplast function ultimately results in parasite death.

Our data do not support primary action of doxycycline against the mitochondrion, as transcription within this organelle and replication of the mitochondrial genome were not obviously altered over two parasite life cycles. Mitochondria also appeared to

segregate normally in the presence of doxycycline, and in the progeny of doxycycline-treated parasites, mitochondria elongated and formed elaborately branched structures similar to those of untreated parasites. We did not observe segregation of these mitochondria at the end of the second cycle, consistent with previous observations that apicoplast segregation always precedes mitochondrial segregation in healthy parasites [24]. However, parasites at this stage displayed gross morphological abnormalities, so lack of mitochondrial segregation was likely secondary to loss of apicoplast function.

In addition to data from plasmodia, there is evidence that prokaryotic protein synthesis inhibitors target the apicoplast of the related apicomplexan parasite *Toxoplasma gondii* [44, 45]. In *T. gondii*, treatment with clindamycin causes a "delayed-death" phenotype in which progeny are able to invade new host cells but die shortly thereafter. A similar phenotype was observed in *T. gondii* parasites that were unable to inherit an apicoplast due to a genetic-segregation defect, leading to the proposal that the apicoplast is required for the establishment of the parasitophorous vacuole. We have observed that *P. falciparum* parasites containing defective apicoplasts survive until the end of their cycle, arguing against a role in establishing the parasitophorous vacuole. This observation is in agreement with ultrastructural studies on the progeny of clindamycin-treated *T. gondii* parasites, which also contain multiple nuclei and appear unable to complete cell division [44]. In both species, death coincides with the initiation of cell division, which occurs early in the *T. gondii* cycle and late in the *P. falciparum* cycle. We propose that the apicoplast is required for the formation of daughter cell plasma membranes, since fatty acid biosynthesis is a likely function of apicoplasts and since our ultrastructural studies indicated that these structures were lacking following doxycycline treatment.

Since doxycycline needs to be administered only transiently to disrupt apicoplast function in the following cycle and since parasites containing nonfunctional apicoplasts can survive for nearly 48 h, doxycycline-treated plasmodia are an ideal model system for probing specific functions of the apicoplast.

Acknowledgements

We thank Geoff McFadden for the ACP_I-GFP and the CS_I-YFP/ACP_I-DsRed transgenic *Plasmodium falciparum* lines, the UCSF Core Cell Imaging Facility for help with electron microscopy, and Julie Lehman, Jamie Koo, Sarah Baxter, and Kevin Lee for excellent technical assistance.

This work was supported by grants from the National Institutes of Health (AI051800 to P.J.R. and AI053862 to J.L.D.), the Medicines for Malaria Venture, the Burroughs Wellcome Fund, and the David and Lucille Packard Foundation. E.L.D. is supported by T32 A1060537. P.J.R. is a Doris Duke Charitable Foundation Distinguished Clinical Scientist.

References

1. Breman JG: **The ears of the hippopotamus: manifestations, determinants, and estimates of the malaria burden**. *Am J Trop Med Hyg* 2001, **64**(1-2 Suppl):1-11.
2. Snow RW, Guerra CA, Noor AM, Myint HY, Hay SI: **The global distribution of clinical episodes of Plasmodium falciparum malaria**. *Nature* 2005, **434**(7030):214-217.
3. Baird JK: **Effectiveness of antimalarial drugs**. *N Engl J Med* 2005, **352**(15):1565-1577.
4. Ryan ET, Kain KC: **Health advice and immunizations for travelers**. *N Engl J Med* 2000, **342**(23):1716-1725.
5. Geary TG, Jensen JB: **Effects of antibiotics on Plasmodium falciparum in vitro**. *Am J Trop Med Hyg* 1983, **32**(2):221-225.
6. Walsh C: **Antibiotics: actions, origins, resistance**. Washington D.C.: ASM Press; 2003.
7. Budimulja AS, Syafruddin, Tapchaisri P, Wilairat P, Marzuki S: **The sensitivity of Plasmodium protein synthesis to prokaryotic ribosomal inhibitors**. *Mol Biochem Parasitol* 1997, **84**(1):137-141.
8. Kiatfuengfoo R, Suthiphongchai T, Prapunwattana P, Yuthavong Y: **Mitochondria as the site of action of tetracycline on Plasmodium falciparum**. *Mol Biochem Parasitol* 1989, **34**(2):109-115.
9. Prapunwattana P, O'Sullivan WJ, Yuthavong Y: **Depression of Plasmodium falciparum dihydroorotate dehydrogenase activity in in vitro culture by tetracycline**. *Mol Biochem Parasitol* 1988, **27**(2-3):119-124.
10. Kohler S, Delwiche CF, Denny PW, Tilney LG, Webster P, Wilson RJ, Palmer JD, Roos DS: **A plastid of probable green algal origin in Apicomplexan parasites**. *Science* 1997, **275**(5305):1485-1489.
11. Williamson DH, Gardner MJ, Preiser P, Moore DJ, Rangachari K, Wilson RJ: **The evolutionary origin of the 35 kb circular DNA of Plasmodium falciparum: new evidence supports a possible rhodophyte ancestry**. *Mol Gen Genet* 1994, **243**(2):249-252.
12. Feagin JE, Werner E, Gardner MJ, Williamson DH, Wilson RJ: **Homologies between the contiguous and fragmented rRNAs of the two Plasmodium falciparum extrachromosomal DNAs are limited to core sequences**. *Nucleic Acids Res* 1992, **20**(4):879-887.
13. Wilson RJ, Denny PW, Preiser PR, Rangachari K, Roberts K, Roy A, Whyte A, Strath M, Moore DJ, Moore PW *et al*: **Complete gene map of the plastid-like DNA of the malaria parasite Plasmodium falciparum**. *J Mol Biol* 1996, **261**(2):155-172.
14. Bender A, van Dooren GG, Ralph SA, McFadden GI, Schneider G: **Properties and prediction of mitochondrial transit peptides from Plasmodium falciparum**. *Mol Biochem Parasitol* 2003, **132**(2):59-66.

15. Foth BJ, Ralph SA, Tonkin CJ, Struck NS, Fraunholz M, Roos DS, Cowman AF, McFadden GI: **Dissecting apicoplast targeting in the malaria parasite Plasmodium falciparum**. *Science* 2003, **299**(5607):705-708.
16. Gardner MJ, Hall N, Fung E, White O, Berriman M, Hyman RW, Carlton JM, Pain A, Nelson KE, Bowman S *et al*: **Genome sequence of the human malaria parasite Plasmodium falciparum**. *Nature* 2002, **419**(6906):498-511.
17. Ralph SA, van Dooren GG, Waller RF, Crawford MJ, Fraunholz MJ, Foth BJ, Tonkin CJ, Roos DS, McFadden GI: **Tropical infectious diseases: metabolic maps and functions of the Plasmodium falciparum apicoplast**. *Nat Rev Microbiol* 2004, **2**(3):203-216.
18. Waller RF, Keeling PJ, Donald RG, Striepen B, Handman E, Lang-Unnasch N, Cowman AF, Besra GS, Roos DS, McFadden GI: **Nuclear-encoded proteins target to the plastid in Toxoplasma gondii and Plasmodium falciparum**. *Proc Natl Acad Sci U S A* 1998, **95**(21):12352-12357.
19. Wilson RJ: **Parasite plastids: approaching the endgame**. *Biol Rev Camb Philos Soc* 2005, **80**(1):129-153.
20. Vaidya AB, Mather MW: **A post-genomic view of the mitochondrion in malaria parasites**. *Curr Top Microbiol Immunol* 2005, **295**:233-250.
21. Trager W, Jenson JB: **Cultivation of malarial parasites**. *Nature* 1978, **273**(5664):621-622.
22. Lambros C, Vanderberg JP: **Synchronization of Plasmodium falciparum erythrocytic stages in culture**. *J Parasitol* 1979, **65**(3):418-420.
23. Waller RF, Reed MB, Cowman AF, McFadden GI: **Protein trafficking to the plastid of Plasmodium falciparum is via the secretory pathway**. *Embo J* 2000, **19**(8):1794-1802.
24. van Dooren GG, Marti M, Tonkin CJ, Stimmler LM, Cowman AF, McFadden GI: **Development of the endoplasmic reticulum, mitochondrion and apicoplast during the asexual life cycle of Plasmodium falciparum**. *Mol Microbiol* 2005, **57**(2):405-419.
25. Desjardins RE, Canfield CJ, Haynes JD, Chulay JD: **Quantitative assessment of antimalarial activity in vitro by a semiautomated microdilution technique**. *Antimicrob Agents Chemother* 1979, **16**(6):710-718.
26. Harlow E, Lane D: **Antibodies: a laboratory manual**. Cold Spring Harbor, N.Y.: Cold Spring Harbor Laboratory; 1988.
27. Bozdech Z, Zhu J, Joachimiak MP, Cohen FE, Pulliam B, DeRisi JL: **Expression profiling of the schizont and trophozoite stages of Plasmodium falciparum with a long-oligonucleotide microarray**. *Genome Biol* 2003, **4**(2):R9.
28. Bozdech Z, Llinas M, Pulliam BL, Wong ED, Zhu J, DeRisi JL: **The transcriptome of the intraerythrocytic developmental cycle of Plasmodium falciparum**. *PLoS Biol* 2003, **1**(1):E5.
29. Eisen MB, Spellman PT, Brown PO, Botstein D: **Cluster analysis and display of genome-wide expression patterns**. *Proc Natl Acad Sci U S A* 1998, **95**(25):14863-14868.
30. Sijwali PS, Shenai BR, Gut J, Singh A, Rosenthal PJ: **Expression and characterization of the Plasmodium falciparum haemoglobinase falcipain-3**. *Biochem J* 2001, **360**(Pt 2):481-489.

31. Thummel KE, Shen DD: **Design and optimization of dosage regimens: pharmacokinetic data**. In: *Goodman and Gilman's the pharmocological basis of therapeutics.* Edited by Hardman JG, Limbird LE, Gilman AG, 10th edn. New York, N.Y.: McGraw-Hill; 2001: 1917-2023.
32. Pradines B, Rogier C, Fusai T, Mosnier J, Daries W, Barret E, Parzy D: **In vitro activities of antibiotics against Plasmodium falciparum are inhibited by iron**. *Antimicrob Agents Chemother* 2001, **45**(6):1746-1750.
33. O'Rourke SM, Herskowitz I: **A third osmosensing branch in Saccharomyces cerevisiae requires the Msb2 protein and functions in parallel with the Sho1 branch**. *Mol Cell Biol* 2002, **22**(13):4739-4749.
34. O'Rourke SM, Herskowitz I: **Unique and redundant roles for HOG MAPK pathway components as revealed by whole-genome expression analysis**. *Mol Biol Cell* 2004, **15**(2):532-542.
35. Kim CC, Falkow S: **Significance analysis of lexical bias in microarray data**. *BMC Bioinformatics* 2003, **4**:12.
36. Preiser PR, Wilson RJ, Moore PW, McCready S, Hajibagheri MA, Blight KJ, Strath M, Williamson DH: **Recombination associated with replication of malarial mitochondrial DNA**. *Embo J* 1996, **15**(3):684-693.
37. Smeijsters LJ, Zijlstra NM, de Vries E, Franssen FF, Janse CJ, Overdulve JP: **The effect of (S)-9-(3-hydroxy-2-phosphonylmethoxypropyl) adenine on nuclear and organellar DNA synthesis in erythrocytic schizogony in malaria**. *Mol Biochem Parasitol* 1994, **67**(1):115-124.
38. Williamson DH, Preiser PR, Moore PW, McCready S, Strath M, Wilson RJ: **The plastid DNA of the malaria parasite Plasmodium falciparum is replicated by two mechanisms**. *Mol Microbiol* 2002, **45**(2):533-542.
39. Divo AA, Geary TG, Jensen JB, Ginsburg H: **The mitochondrion of Plasmodium falciparum visualized by rhodamine 123 fluorescence**. *J Protozool* 1985, **32**(3):442-446.
40. Sato S, Rangachari K, Wilson RJ: **Targeting GFP to the malarial mitochondrion**. *Mol Biochem Parasitol* 2003, **130**(2):155-158.
41. van Dooren GG, Su V, D'Ombrain MC, McFadden GI: **Processing of an apicoplast leader sequence in Plasmodium falciparum and the identification of a putative leader cleavage enzyme**. *J Biol Chem* 2002, **277**(26):23612-23619.
42. Divo AA, Geary TG, Jensen JB: **Oxygen- and time-dependent effects of antibiotics and selected mitochondrial inhibitors on Plasmodium falciparum in culture**. *Antimicrob Agents Chemother* 1985, **27**(1):21-27.
43. Lin Q, Katakura K, Suzuki M: **Inhibition of mitochondrial and plastid activity of Plasmodium falciparum by minocycline**. *FEBS Lett* 2002, **515**(1-3):71-74.
44. Camps M, Arrizabalaga G, Boothroyd J: **An rRNA mutation identifies the apicoplast as the target for clindamycin in Toxoplasma gondii**. *Mol Microbiol* 2002, **43**(5):1309-1318.
45. Fichera ME, Roos DS: **A plastid organelle as a drug target in apicomplexan parasites**. *Nature* 1997, **390**(6658):407-409.

Figure 1. Delayed effects of doxycycline are stage dependent. Highly synchronized parasites were treated with doxycycline for different intervals during a single life cycle, as indicated by the black shading. Parasitemias (% control) were determined 48 or 96 h after the start of the experiment. Note that inhibitory effects of doxycycline were much greater after two cycles (results with >50% inhibition are in boldface), even though the drug was removed after the first cycle.

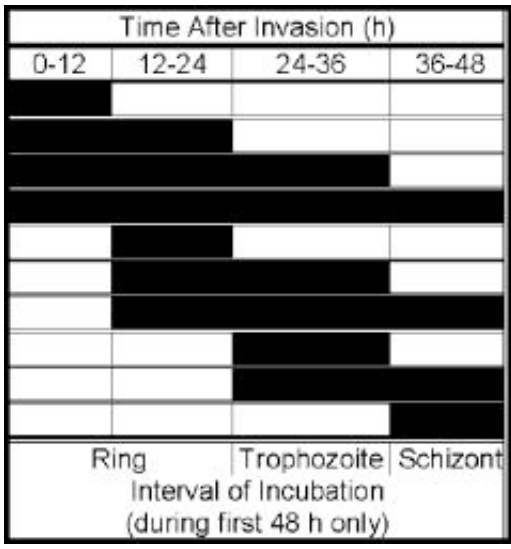

% Control Parasitemia					
48 h			96 h		
92	83	84	95	88	84
100	70	60	95	52	**29**
100	74	**45**	**30**	**15**	**3**
100	70	39	**13**	**9**	**0**
100	90	98	100	73	**39**
98	75	**33**	**34**	**14**	**3**
97	68	**42**	**11**	**9**	**1**
100	86	51	**39**	**14**	**3**
90	78	38	**13**	**10**	**1**
98	90	71	100	60	**12**
1	3	10	1	3	10
Doxycycline Concentration (μM)					

Figure 2. Doxycycline causes morphological abnormalities late in the second cycle of treatment. Synchronized parasites were treated with 1 μM doxycycline or 0.1% DMSO (control) over two life cycles, beginning at the early ring stage (0 h). (A) Parasites were analyzed every 8 h by light microscopy of Giemsa-stained smears. (B) Parasites at 40 and 88 h were analyzed by electron microscopy.

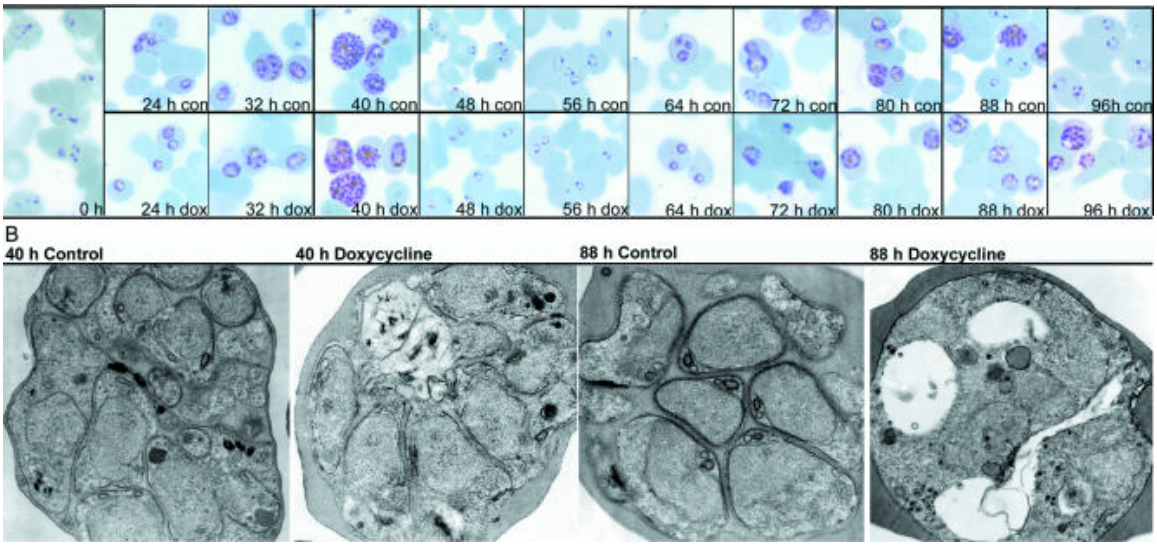

Figure 3. Transcriptome analysis of doxycycline-treated parasites reveals lower mRNA abundance of apicoplast genes. Early trophozoites (approximately 20 h postinvasion) were treated with 1 μM doxycycline or 0.1% DMSO for 20 h and then transferred to drug-free media and cultured for an additional 35 h. RNA was isolated from samples collected every 5 h, converted into labeled cDNA, and hybridized to a 70-mer-based microarray as previously described [28]. (A) Expression data from an overview set of 3,721 oligonucleotide features were plotted according to the phase of expression, derived from previous analysis [28]. Increased expression is shown in red, and decreased expression in green. (B) For plastid genes, excluding tRNAs, the ratio of underexpresssion was plotted in yellow. (C) A histogram of the ratio between treated and untreated parasites at the final time point was plotted. The positions and numbers of plastid genes, excluding tRNAs, are shown as red dots.

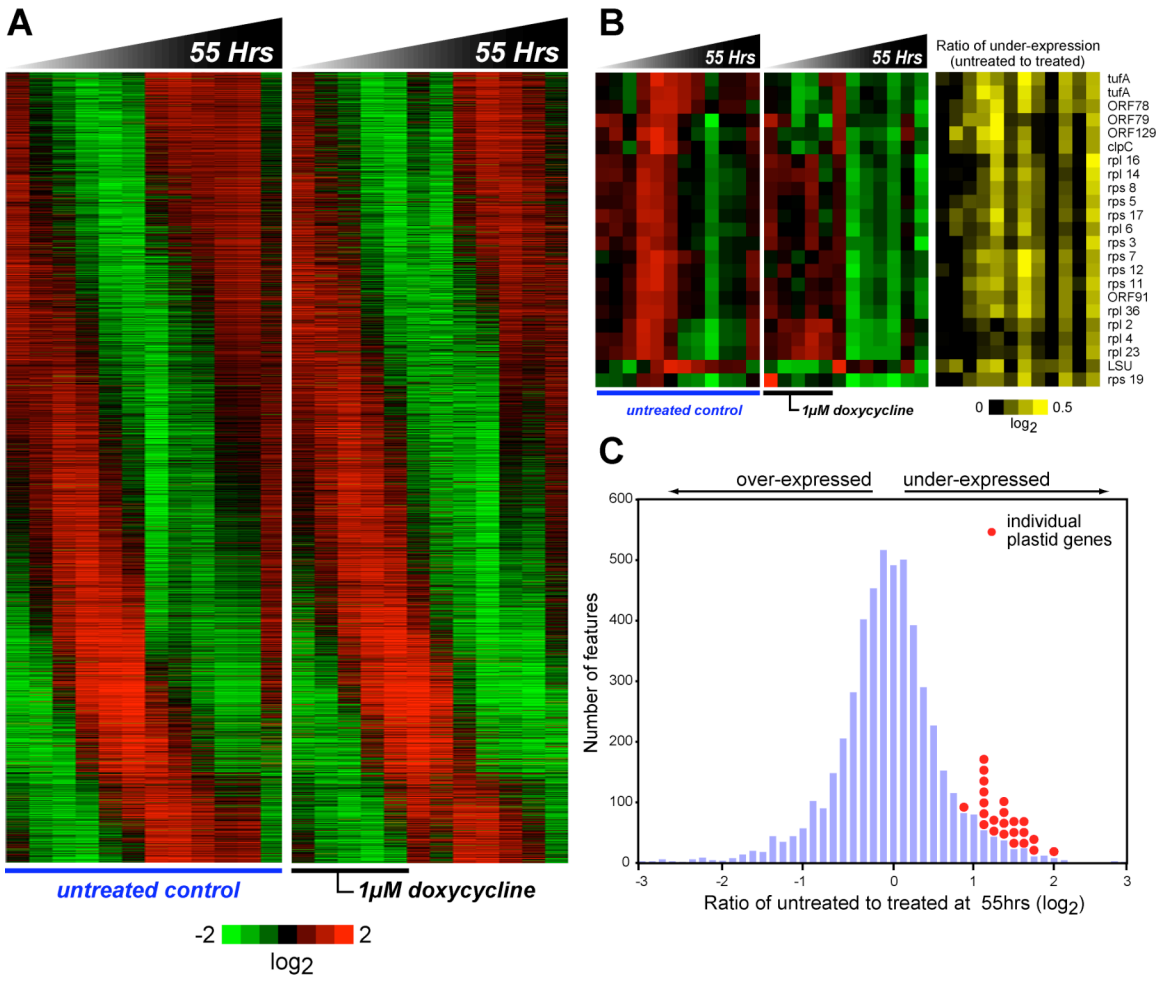
A
55 Hrs
55 Hrs
untreated control
1μM doxycycline
-2
2
log2
B
55 Hrs
55 Hrs
Ratio of under-expression
(untreated to treated)
tufA
tufA
ORF78
ORF79
ORF129
clpC
rpl 16
rpl 14
rps 8
rps 5
rps 17
rpl 6
rps 3
rps 7
rps 12
rps 11
ORF91
rpl 36
rpl 2
rpl 4
rpl 23
LSU
rps 19
untreated control
1μM doxycycline
0
0.5
log2
C
over-expressed
under-expressed
individual
plastid genes
Number of features
600
500
400
300
200
100
0
-3
-2
-1
0
1
2
3
Ratio of untreated to treated at 55hrs (log2)

Figure 4. Replication of the apicoplast genome was blocked in the progeny of doxycycline-treated parasites. Parasites were treated with 1 μM doxycycline (Dox) or 0.1% DMSO (C) for 24 h, beginning at the late ring stage, and then subcultured into fresh medium and allowed to continue a second cycle in the absence of drugs. Schizonts were collected during both the first and second cycles, DNA was extracted, and Southern hybridizations were performed using DNA probes for apicoplast, mitochondrial, and nuclear genomic sequences. The positions of molecular size markers are indicated.

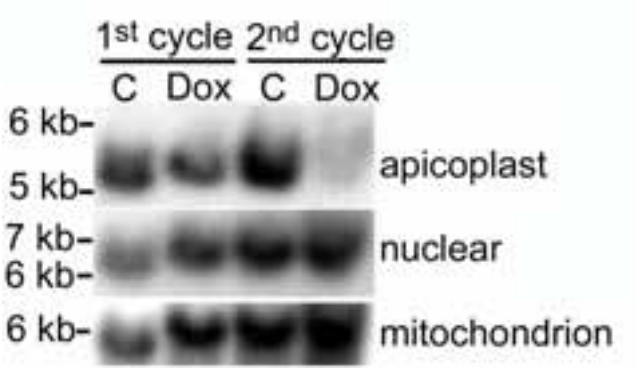

Figure 5. Development of the apicoplast is blocked in the progeny of doxycycline-treated parasites. Parasites stably expressing the apicoplast-targeted ACP_I-GFP transgene were treated with 1 μM doxycycline or 0.1% DMSO as described in the legend to Fig. 4. Parasites were analyzed by fluorescence microscopy at trophozoite (T), early schizont (ES), and late schizont (LS) stages. The apicoplast appears green; nuclei are stained blue with DAPI.

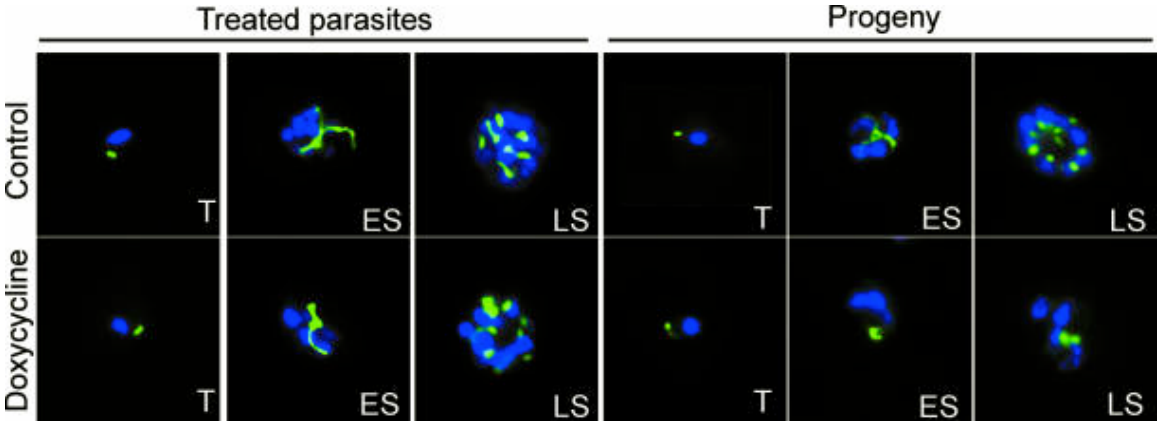

Figure 6. The mitochondrion elongates and branches normally but is unable to segregate in the progeny of doxycycline-treated parasites. Dually transfected parasites expressing the mitochondrion-targeted CS_l-YFP transgene and the apicoplast-targeted ACP_l-DsRed transgene were treated with 1 μM doxycycline or 0.1% DMSO and analyzed as described in the legend to Fig. 5. Trophozoite (T), early schizont (ES), and late schizont (LS) stages are shown. The mitochondrion appears green, and the apicoplast appears red.

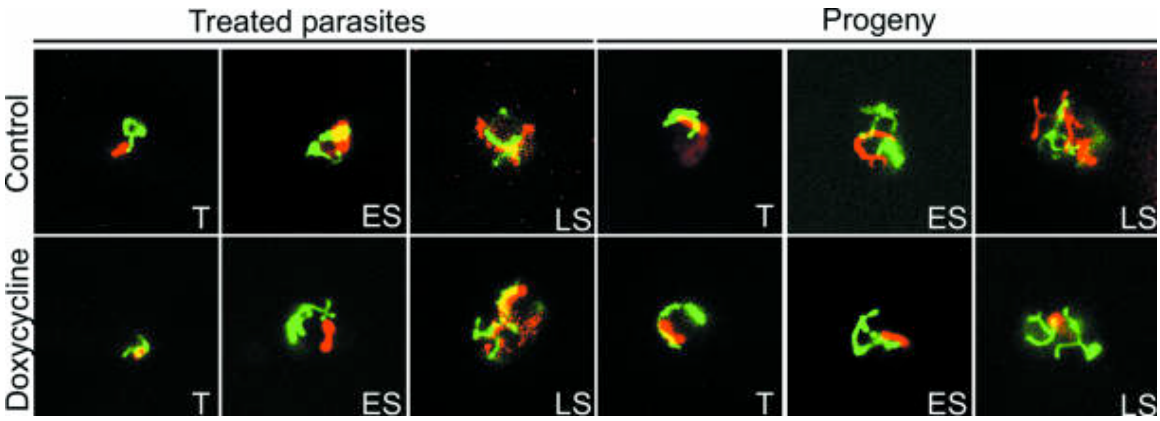

Figure 7. Apicoplast protein processing is inhibited in the progeny of doxycycline-treated parasites. Proteins from doxycycline-treated and control parasites, treated as described in the legend to Fig. 5, were analyzed by immunoblotting with anti-GFP and anti-falcipain-3 (FP-3) antibodies. The locations of proteins and the positions of molecular mass markers (kDa) are indicated.

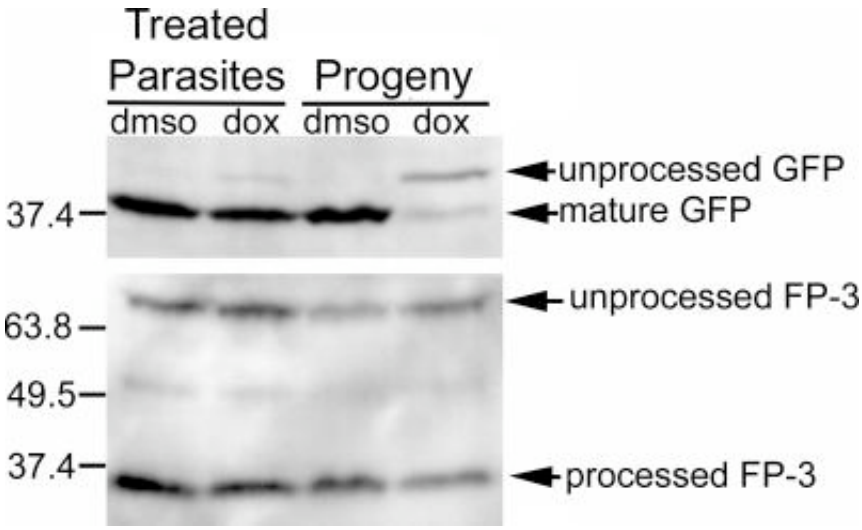

Table 1. W2-strain parasites were incubated with drugs for 48 h, beginning at the late ring stage, and then analyzed or cultured for an additional 48 h in the absence of drugs before analysis. Ring stage parasitemias were determined by counting YOYO-1-stained infected erythrocytes by flow cytometry. Metabolic activity was assessed by quantitation of [^{3}H]hypoxanthine uptake. IC_{50}s are means ± standard errors of the mean from two independent experiments, each performed in duplicate.

Time of Assay	**IC_{50} (μM)**			
Parasite counts	**Doxycycline**	**Minocycline**	**Tetracycline**	**Chloroquine**
48 h	4.8 ± 0.2	4.6 ± 0.2	22.3 ± 0.5	0.10 ± 0.02
96 h	0.46 ± .07	0.14 ± 0.03	0.45 ± .01	0.083 ± 0.012
Hypoxanthine Uptake	**Doxycycline**	**Minocycline**	**Tetracycline**	**Chloroquine**
48 h	16.0 ± 3.0	10.8 ± 1.3	51.0 ± 1.0	0.13 ± 0.03
96 h	1.02 ± 0.24	0.35 ± 0.08	1.27 ± 0.53	0.073 ± 0.006

Chapter 4: Using *Saccharomyces cerevisiae* as a heterologous system to study the structure-function relationship of the *Plasmodium falciparum* chloroquine resistance transporter

Introduction

Plasmodium falciparum, one of the four strains that cause malaria in humans continues to be a major cause of morbidity and mortality in much of the world [1]. Because of widespread resistance to the most commonly used drugs, deaths from malaria have actually increased in the last decade [2]. Beginning during the Second World War, chloroquine was used extensively and proved to be a safe and effective treatment for malaria infection. However, widespread resistance began appearing and quickly spread across the world by the 1970s. The gene responsible for this resistance was mapped to the *Plasmodium falciparum* chloroquine resistance transporter (PfCRT) [3, 4].

Although extensive work has been done to characterize PfCRT and to determine what causes the resistance phenotype, the mechanism remains unclear. It is also unclear how this resistance to chloroquine may affect the speed of acquired resistance for other related drugs. There are many highly potent 4-amino-quinolines currently in development which bypass resistance *in vitro*[5-7]. However it is unclear whether resistance *in vivo* will arise rapidly to these drugs because of their similarity to chloroquine, or whether they will continue to bypass resistance due to chloroquine resistant alleles of PfCRT.

Choosing drugs which bypass resistance caused by mutations in PfCRT may help extend the period of efficacy after the drug is started in clinical use. To help choose only

those drugs that bypass resistance, a method for high-throughput screening of resistance profiles to these drugs is needed. One way to do this is to select for resistance *in vitro* through continuous drug pressure on cultured strains. However, because of the difficulty of culturing *P. falciparum* for extended periods of time, this approach is not amenable to high-throughput screening of drug libraries. Another option is to first use a heterologous system to screen drugs for their efficacy against sensitive and resistant alleles of PfCRT, and immediately discard any that are not effective against resistant alleles.

To reach this goal, we have expressed a recoded version of PfCRT in *Saccharomyces cerevisiae*. *S. cerevisiae* is amenable to genetic manipulation, has a fast doubling time, and has been extensively studied so that a large base of knowledge is already present. Additionally, a large number of invaluable tools have been generated for yeast such as knock-out libraries and GFP-tagged libraries. However, because *S. cerevisiae* is naturally extremely resistant to chloroquine, we have first focused on sensitizing the system so that small differences between resistant and sensitive alleles of PfCRT can be observed. One way to find a more sensitive readout is to use microarrays to look for genes with a strong response to chloroquine. These genes also need to have a distinguishable response between strains expressing sensitive and resistant alleles of PfCRT. These small differences in response could then be magnified through use of engineered promoters driving specific reporters or selection markers.

Results

To determine if *S. cerevisiae* has a transcriptional response to chloroquine, we used microarrays to look at gene expression in yeast cultures treated with 0, 25, 50, 100,

or 200 mM chloroquine for one hour. The results of these experiments are shown in Figure 1. Because we are interested in finding promoters with strong up-regulation in response to chloroquine, we focused on the cluster of genes that is up-regulated in a dose-dependent manner. This group of 541 genes is shown in more detail in Figure 1A. Using GoStat analysis to look for over-represented gene ontology terms, we found that this cluster is highly enriched for genes involved in processes related to the vacuole and cell wall [8]. This is not surprising considering previous work showing that deleting components of the cell-wall integrity sensor sensitizes yeast to chloroquine (V. Newman, unpublished results), and that PfCRT is localized to the vacuole in yeast (V. Newman, M. Alexander, unpublished results). The genes were sorted according to fold change over the cultures treated with 0 chloroquine and the top 10 are shown in Figure 1B. These genes show a robust dose dependent and linear response to chloroquine treatment. Again, these genes are involved mainly in processes associated with the cell wall including Tir1 and Tir2, which are transcribed in response to anaerobic stress, and Pir1, Pir3, Pst1 and Mid2 which are components of or regulated by the cell-wall integrity sensor.

Next, we determined whether strains with resistant (Dd2) or sensitive (HB3) alleles of PfCRT had a similar response to chloroquine. We also wished to find genes with a distinguishably different response between the resistant and sensitive alleles. In preliminary results, it appears that strains with the sensitive allele behave more similarly to strains with no PfCRT, while strains with the resistant allele have a less robust response to chloroquine. A cluster containing several of the most up-regulated genes in the wild-type strain are shown in Figure 2. The highest response to chloroquine is seen in

the wild-type strain, the HB3 allele of PfCRT has an intermediate response, and the Dd2 allele of PfCRT has no discernible response.

Discussion

We have shown that *S. cerevisiae* clearly responds to chloroquine treatment, and that this response is moderated by the expression of PfCRT. A subset of cell wall associated genes has a distinguishable response depending on the resistance status of the PfCRT allele expressed. These genes are good candidates for future experiments in which their promoters can be engineered to increase sensitivity and to drive reporters or selective markers for high-throughput screening. For instance, the regulation of the mannoprotein genes including Tir1 and Tir2 has been worked out in *S. cerevisiae* [9, 10]. These genes are activated by Mox4 which binds to an 8 base pair consensus sequence termed the anaerobic response element 1 (AR1). A construct could be engineered which drives a reporter and contains multiple AR1 sites to increase the sensitivity of the chloroquine response. This construct can also be introduced into strains with gene deletions which cause higher chloroquine sensitivity to further sensitize the assay. Deletions in several components of the cell wall integrity sensor such as Rgd1 and Mid1 cause an increase in chloroquine sensitivity (V. Newman, unpublished results).

Using this system, in which sensitive and resistant alleles of PfCRT can be easily distinguished, many different point mutations can be screened for resistant or sensitive behavior to determine a structure-function relationship for PfCRT. Once a structure-function relationship is determined for PfCRT, new 4-amino-quinolines can be quickly screened in this system. We can then determine if point mutations in regions of PfCRT

known to cause resistance to chloroquine can also cause resistance to the new drugs, and choose only those that bypass known resistance mechanisms in PfCRT.

Materials and Methods

Yeast strains and culture conditions

All experiments were carried out in strain BY4741. PfCRT from either the HB3 or Dd2 allele was integrated at the *ADE2* locus and driven by *pGal1-10*. *RGD1* was deleted by integration of the *kanMX* cassette into that locus. All strains were grown in minimal medium (YNB) with 400 mM H_3PO_4, which corresponds to the amount of phosphoric acid in a solution of 200 mM chloroquine diphosphate (Sigma).

Cultures were grown overnight to around OD600=0.4 in 2% raffinose, 0.05% dextrose minimal medium with complete amino acids plus high adenine and phosphoric acid. These cultures were then diluted into 1L cultures in minimal medium with phosphoric acid, complete amino acids with high adenine, and 2% galactose for a 4 hour induction, at 30° C, with shaking. After induction, the cells were harvested by centrifugation at 4500 rpm for 5 minutes and resuspended in water before dispensing into 500 mL aliquots of medium (S-gal-phosphoric acid, complete amino acids with high adenine containing 0, (5 mM for HB3 and Dd2 experiments) 25, 50, 100, or 200 mM chloroquine). The cultures were incubated at 30° C, with shaking, for 1 hour before collection by filtration, after which the filtered cells were flash-frozen and stored at –80° C until RNA extraction.

Microarray analysis

For each sample, 2 μg of poly(A) selected RNA was reverse transcribed into cDNA containing amino-allyl dUTP (Ambion) using SuperScript II reverse transcriptase (Invitrogen). Each sample of cDNA was then coupled to Cy5 and a pool of cDNAs representing all samples was coupled to Cy3. The Cy5 labeled samples and Cy3 labeled pool were then competitively hybridized to an array containing Operon yeast genome oligo set. Microarrays were scanned using a GenePix 4000A scanner and images were analyzed using GenePix software. The microarray data was then stored and normalized in the NOMAD database (http://ucsf-nomad.sourceforge.net). Expression data were log transformed and median centered and cluster analysis was performed using Cluster software and visualized using Treeview[11].

Gene Ontology analysis was done using the GoStat tool with the following parameters: minimal length of considered GO paths = 3, maximal p-value = 0.01, cluster GOs = -1, correct for multiple testing = none [8].

References

1. Snow RW, Guerra CA, Noor AM, Myint HY, Hay SI: **The global distribution of clinical episodes of Plasmodium falciparum malaria**. *Nature* 2005, **434**(7030):214-217.
2. Yamey G: **Roll Back Malaria: a failing global health campaign**. *Bmj* 2004, **328**(7448):1086-1087.
3. Wellems TE, Panton LJ, Gluzman IY, do Rosario VE, Gwadz RW, Walker-Jonah A, Krogstad DJ: **Chloroquine resistance not linked to mdr-like genes in a Plasmodium falciparum cross**. *Nature* 1990, **345**(6272):253-255.
4. Sidhu AB, Verdier-Pinard D, Fidock DA: **Chloroquine resistance in Plasmodium falciparum malaria parasites conferred by pfcrt mutations**. *Science* 2002, **298**(5591):210-213.
5. Madrid PB, Liou AP, DeRisi JL, Guy RK: **Incorporation of an intramolecular hydrogen-bonding motif in the side chain of 4-aminoquinolines enhances activity against drug-resistant P. falciparum**. *J Med Chem* 2006, **49**(15):4535-4543.
6. Madrid PB, Sherrill J, Liou AP, Weisman JL, Derisi JL, Guy RK: **Synthesis of ring-substituted 4-aminoquinolines and evaluation of their antimalarial activities**. *Bioorg Med Chem Lett* 2005, **15**(4):1015-1018.
7. Madrid PB, Wilson NT, DeRisi JL, Guy RK: **Parallel synthesis and antimalarial screening of a 4-aminoquinoline library**. *J Comb Chem* 2004, **6**(3):437-442.
8. Beissbarth T, Speed TP: **GOstat: find statistically overrepresented Gene Ontologies within a group of genes**. *Bioinformatics* 2004, **20**(9):1464-1465.
9. Abramova NE, Cohen BD, Sertil O, Kapoor R, Davies KJ, Lowry CV: **Regulatory mechanisms controlling expression of the DAN/TIR mannoprotein genes during anaerobic remodeling of the cell wall in Saccharomyces cerevisiae**. *Genetics* 2001, **157**(3):1169-1177.
10. Cohen BD, Sertil O, Abramova NE, Davies KJ, Lowry CV: **Induction and repression of DAN1 and the family of anaerobic mannoprotein genes in Saccharomyces cerevisiae occurs through a complex array of regulatory sites**. *Nucleic Acids Res* 2001, **29**(3):799-808.
11. Eisen MB, Spellman PT, Brown PO, Botstein D: **Cluster analysis and display of genome-wide expression patterns**. *Proc Natl Acad Sci U S A* 1998, **95**(25):14863-14868.

Figure 1. *S. cerevisiae* response to chloroquine treatment. (A) *S. cerevisiae* cultures were treated with 0, 25, 50, 100 or 200 mM chloroquine for 1 hour. The response for all genes is shown on the left and a subset of genes up-regulated by increasing chloroquine concentration is shown in more detail on the right. (B) The 10 genes with the highest fold change over no chloroquine treatment show a fairly dose dependent response to chloroquine treatment.

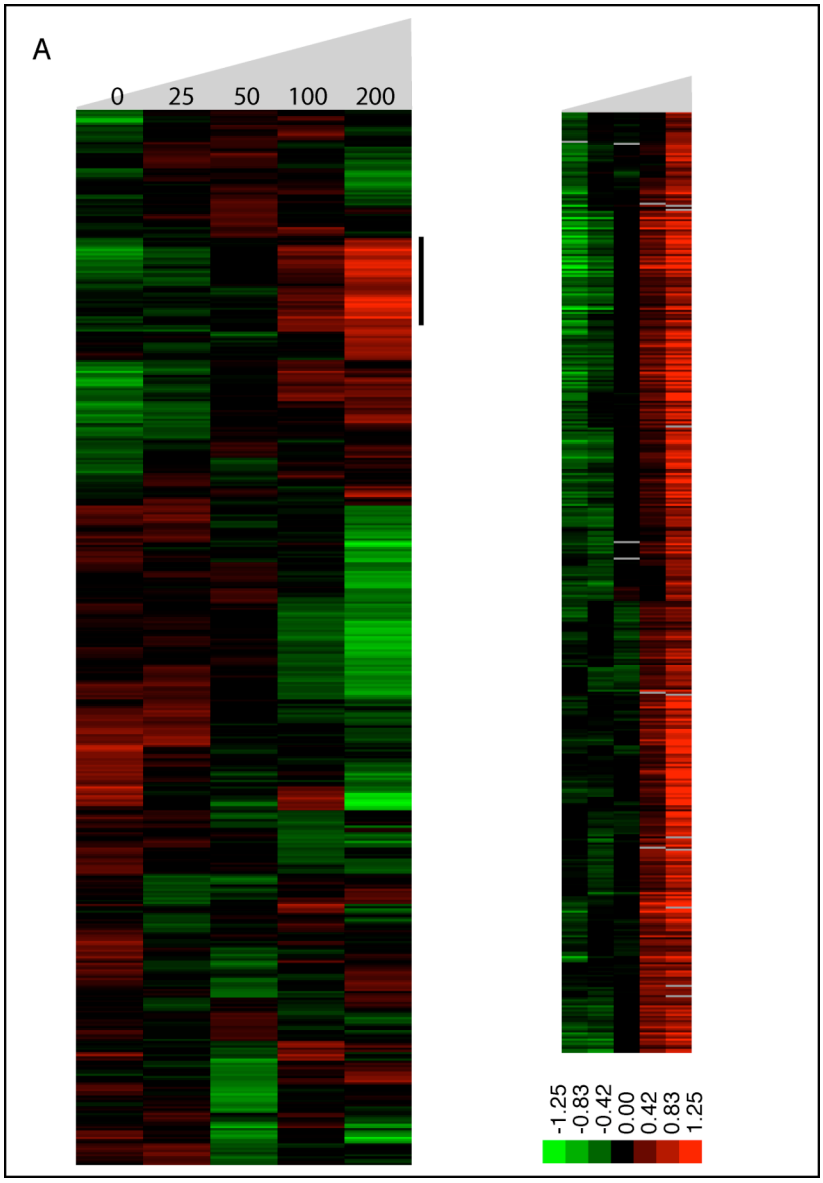

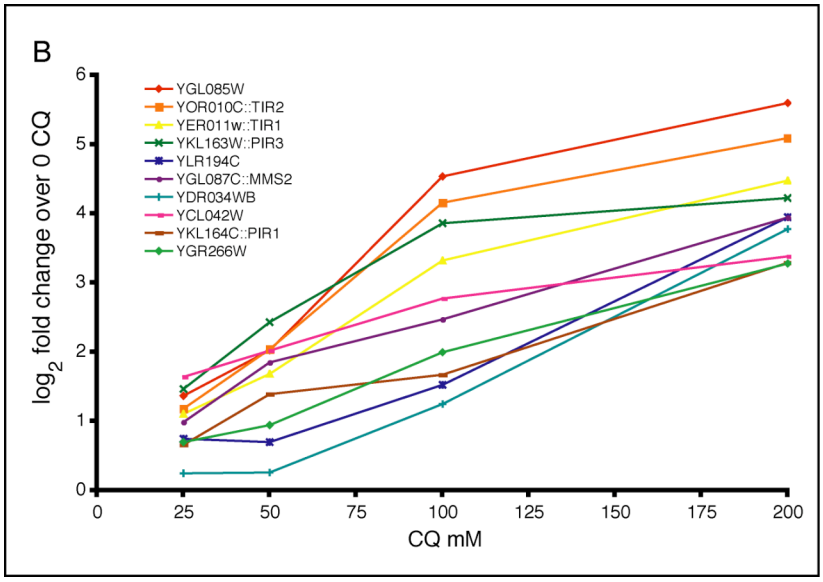
B
log2 fold change over 0 CQ
CQ mM
YGL085W
YOR010C::TIR2
YER011w::TIR1
YKL163W::PIR3
YLR194C
YGL087C::MMS2
YDR034WB
YCL042W
YKL164C::PIR1
YGR266W
0
1
2
3
4
5
6
0
25
50
75
100
125
150
175
200

Figure 2. A subset of genes show a differential response to chloroquine in the sensitive versus the resistant allele of PfCRT.

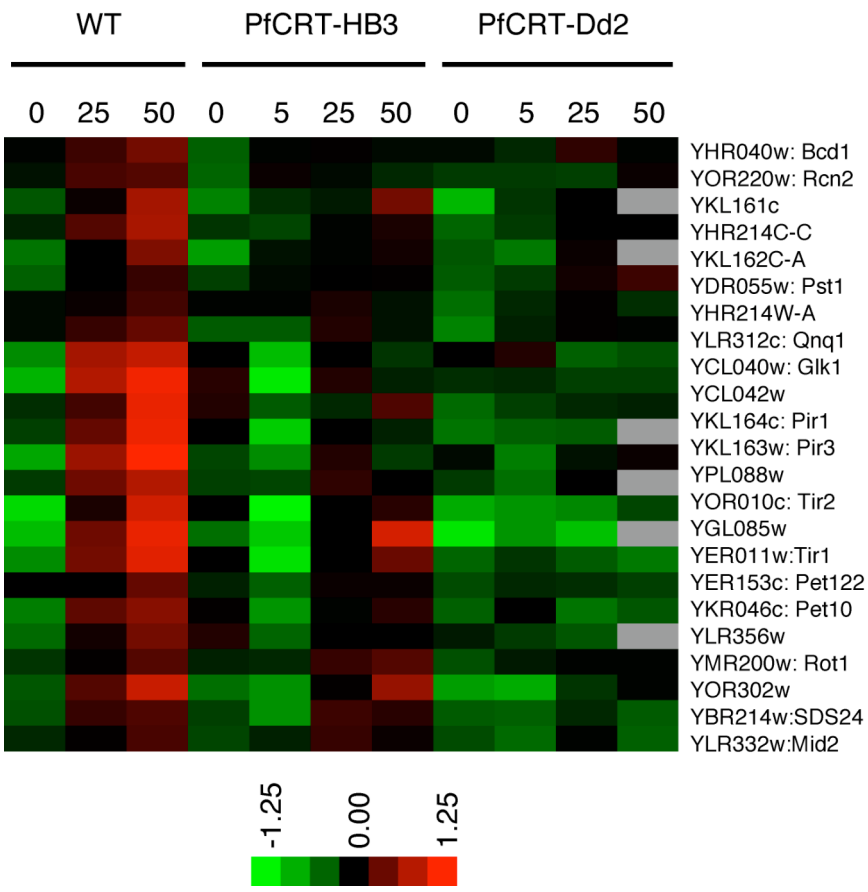

Appendix: Biochemical characterization of mRNA decay activities in *P. falciparum*

Introduction

mRNA decay is an extremely important part of gene regulation in many organisms, but appears to be particularly important in *P. falciparum*. In Chapter 2, we showed that mRNA decay rates appear to be globally regulated during the intra-erythrocytic developmental cycle (IDC). As the parasites move through the IDC, the half-lives for mRNA across the genome lengthen considerably. However, they do not lengthen at the same rate and they can be clustered into similar groups with over-represented functional categories.

The mechanisms behind both the global lengthening of half-lives and the specific decay patterns remain unknown. One simple possibility to explain the global lengthening of half-lives over the life-cycle is a gradual decrase in the amount of a specific decay protein or activity over the course of the life cycle. To test this possibility, we attempted to use *P. falciparum* extracts from different stages along with specific *in vitro* transcribed RNAs to characterize the deadenylation, decapping and exonucleolytic decay activities. Unfortunately, these efforts were hampered by an extremely robust RNase A activity in the media used to grow *P. falciparum in vitro*. This activity could not be easily separated from any possible decay activity in the parasites themselves.

Although this approach proved unsuccessful, many of the techniques we developed for specific labeling of RNAs should be useful if the *P. falciparum* mRNA decay activity can be separated from the contamination, or if specific components of the

decay pathway were expressed and purified from a heterologous system. These techniques involve specific labeling of the body or the RNA, the 5' methyl cap or the poly(A) tail. Using gene synthesis techniques, we could also create specific sequence characteristics to test possible sequence specific differences in any of the mRNA decay steps.

Materials and methods

Body labeled RNA

RNA used for general detection of RNase activity was labeled throughout the transcript. The steps for the synthesis of this type of transcript are diagrammed in Figure 1A. DNA templates were amplified from the genome using a forward primer with the minimal t7 promoter (TAATACGACTCACTATAGGG) added on the 5' end. The PCR products were then purified using Zymo columns. *in vitro* transcription reactions were carried out using the Ambion MEGAscript high yield transcription kit. The reaction was set up as follows:

1 µg DNA template
1 µL 75 mM ATP
1 µL 75 mM GTP
1 µL 75 mM CTP
0.25 µL 75 mM UTP
2.5 µL [α-^{32}P] UTP (800 Ci/mmol)
1 µL 10x buffer
1 µL t7 polymerase

The reaction was incubated at 37° for 2-4 hours and cleaned with Zymo RNA Clean-up kit-25 as per the manufacturers instructions.

A 5’ methyl cap was then added using the Epicentre Biotechnologies ScriptCap m^7G Capping system using the alternate cap 0 protocol designed for use on 1-10 µg of RNA. The reaction was incubated at 37° for 1 hour.

The entire reaction was then added to the Epicentre Biotechnologies A-Plus Poly(A) Polymerase Tailing Kit to add a poly(A) tail. For poly(A) tails around 60 bp, the A-Plus Poly(A) polymerase added was reduced to 2 units and the reaction was incubated at 37° for 30 minutes.

The reaction was then extracted with phenol: chloroform followed by isopropenol precipitation. The dried RNA was resuspended in 10 µL Ambion gel loading buffer and run on a 5% denaturing polyacrylamide gel. Bands were visualized using autoradiography and excised from the gel. The gel slab was then placed in 400 µL HSCB buffer (25 mM Tris-Cl pH 7.6, 0.1% SDS, 400 mM NaCl) and soaked at room temperature overnight. The RNA was then extracted with phenol: chloroform followed by isopropenol precipitation and resuspended in water at the desired concentration.

Cap labeled RNA

RNA used to investigate decapping and decay from the 5’ end was labeled on the 5’ methyl cap. The steps for the synthesis of this type of transcript are diagrammed in Figure 1B. DNA templates were prepared as described above. The *in vitro* reaction was set up as follows:

1 µg DNA template
1 µL 75 mM ATP
1 µL 75 mM GTP
1 µL 75 mM CTP
1 µL 75 mM UTP
1 µL 10x buffer

1 μL t7 polymerase

The reaction was incubated at 37° for 2-4 hours and cleaned with Zymo RNA Clean-up kit-25 as per the manufacturers instructions.

A 5' methyl cap was then added using the Epicentre Biotechnologies ScriptCap m^7G Capping system using the alternate cap 0 protocol designed for use on 1-10 μg of RNA with a few alterations. In step one the total reaction volume was reduced to 10.5 μL. In step four the 2 μL 10mM GTP was replaced with 5 μL [α-^{32}P] GTP (800 Ci/mmol). The reaction was incubated at 37° for 2 hour.

The reaction then proceeded through poly(A) tailing and clean-up as described above. Decapping assays were performed as described previously [1].

Poly(A) tail labeled RNA

RNA used to investigate deadenylation or decay from the 3' end was labeled specifically on the poly(A) tail. The steps for the synthesis of this type of transcript are diagrammed in Figure 1C. The DNA templates, *in vitro* transcription and Zymo clean-up were carried out as described under cap labeled RNA. The RNA transcript was capped as described under body labeled RNA.

For the poly(A) addition, the 10 μL 10 mM ATP was replaced with 2 μL 10 mM ATP plus 8 μL [α-^{32}P] ATP (3000 Ci/mmol). 2 units A-Plus Poly(A) polymerase up to 8 units A-Plus Poly(A) polymerase were used. This reaction was allowed to proceed 30 minutes to 2 hours depending on the length of tail desired which can be titrated based on incubation time, poly(A) polymerase concentration and reaction volume. These reactions were purified as described above.

Gene synthesis

In order to have DNA templates with specific sequence characteristics, some genes were synthesized. The oligos were designed using the Gene2oligo program [2]. The first and second round PCRs were also performed as described.

References

1. Bergman N, Opyrchal M, Bates EJ, Wilusz J: **Analysis of the products of mRNA decapping and 3'-to-5' decay by denaturing gel electrophoresis**. *Rna* 2002, **8**(7):959-965.
2. Rouillard JM, Lee W, Truan G, Gao X, Zhou X, Gulari E: **Gene2Oligo: oligonucleotide design for in vitro gene synthesis**. *Nucleic Acids Res* 2004, **32**(Web Server issue):W176-180.

Figure 1. : Diagram of the steps to synthesize body labeled, cap labeled and poly(A) tail labeled RNA. In each panel the orange stars represent nucleotides that have been radiolabeled. Panel A represents the steps to body label, panel B to cap label and panel C to poly(A) tail label.

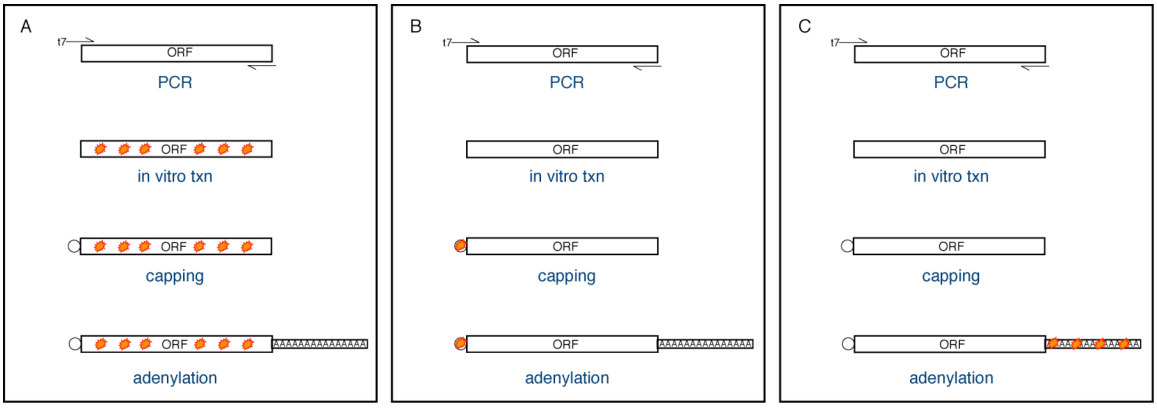

Publishing Agreement

It is the policy of the University to encourage the distribution of all theses and dissertations. Copies of all UCSF theses and dissertations will be routed to the library via the Graduate Division. The library will make all theses and dissertations accessible to the public and will preserve these to the best of their abilities, in perpetuity.

I hereby grant permission to the Graduate Division of the University of California, San Francisco to release copies of my thesis or dissertation to the Campus Library to provide access and preservation, in whole or in part, in perpetuity.

Author Signature Date